frontiers | Frontiers in Marine Science

TYPE Original Research
PUBLISHED 13 November 2024
DOI 10.3389/fmars.2024.1426906

OPEN ACCESS

EDITED BY
Douglas G Capone,
University of Southern California,
United States

REVIEWED BY
Peter Leslie Croot,
University of Galway, Ireland
Randelle M Bundy,
University of Washington, United States

*CORRESPONDENCE
Gemma Portlock
g.l.portlock@soton.ac.uk
Pascal Salaün
salaun@liverpool.ac.uk

RECEIVED 02 May 2024
ACCEPTED 11 September 2024
PUBLISHED 13 November 2024

CITATION
Portlock G, Whitby H and Salaün P (2024) Distribution and behaviour of reduced sulfur substances in the oligotrophic and hydrothermal waters of the Western Tropical South Pacific.
Front. Mar. Sci. 11:1426906.
doi: 10.3389/fmars.2024.1426906

Distribution and behaviour of reduced sulfur substances in the oligotrophic and hydrothermal waters of the Western Tropical South Pacific

Gemma Portlock[1,2*], Hannah Whitby[2] and Pascal Salaün[2*]

[1]School of Ocean and Earth Science, National Oceanography Centre Southampton, University of Southampton, Southampton, United Kingdom, [2]Department of Earth, Ocean and Ecological Sciences, School of Environmental Sciences, University of Liverpool, Liverpool, United Kingdom

Reduced sulfur species (RSS) are involved in essential biological and chemical processes, including metal complexation, yet little is known about their occurrence and behaviour in marine systems. Here, we present a quantitative and qualitative data set of species-specific RSS in open ocean samples collected during the GEOTRACES Tonga GPpr14 cruise. The cruise traversed differing biogeochemical provinces, from the mesotrophic Melanesian waters and the North Fiji Basin, through the hydrothermally active Lau Basin, eastward to the oligotrophic South Pacific Gyre. Using cathodic stripping voltammetry in acidified samples (pH 2), we measured the concentration of two RSS, with peak potentials of -0.18 and -0.09 V in equivalents of thioacetamide (TA) and glutathione (GSH) respectively. GSH-like compounds were only present in the upper 200 m at concentrations up to 6.2 nM eq. GSH, consistent with other cathodic stripping voltammetry as well as chromatography-based studies. In contrast, $RSS^{2}_{-0.18\ V}$ compounds were detected at all depths at concentrations ranging from 48 nM to 980 nM eq. TA. Both $RSS^{2}_{-0.18\ V}$ and GSH-like compounds were present at higher levels in the hydrothermally-impacted region of the Lau Basin relative to other stations. The highest levels, along with high sulfide concentrations, were detected in a hydrothermal plume sample, indicating that hydrothermal vents are a direct or indirect source of these compounds. Elevated levels of $RSS^{2}_{-0.18\ V}$ compounds were detected throughout almost the entire water column at a station located in the North Fiji Basin. We also employed the qualitative technique of cathodic pseudopolarography on unbuffered samples (pH ~ 8.5). Pseudopolarograms of marine RSS were compared to sulfide, GSH and TA standards. Pseudopolarography supports the presence of GSH in marine samples. However, while a compound that is electrochemically similar to TA is often detected in marine samples, TA itself is not thought to be naturally present. This is supported by our pseudopolarograms of $RSS^{8.5}_{-0.52\ V}$ which often lacked the characteristic TA reduction wave but suggested the presence of other unidentified RSS compounds.

KEYWORDS

reduced sulfur substances, thioacetamide, glutathione, sulfide, hydrothermal fluids, Western Tropical South Pacific, pseudopolarography

1 Introduction

The Western Tropical South Pacific (WTSP) is a vast oceanic region that extends from Australia to the western boundary of the South Pacific Gyre. Within the WTSP is the Tonga-Kermadec Arc where the Pacific plate subducts under the Australian plate, causing a region of extensive hydrothermal activity (Baker et al., 2019; German et al., 2006). Hydrothermal vents release both metal and non-metal chemicals, including sulfur, iron, carbon dioxide and methane (Feely et al., 1996; Klinhammer et al., 1977; Klinkhammer et al., 1983; Resing et al., 2015) which play an important role in ocean chemistry. These inputs can influence the biogeochemical cycles of surrounding waters, affecting primary production and nutrient availability (Ardyna et al., 2019; Schine et al., 2021). Recently, attention has been focused on the importance of shallow (<200 m) hydrothermal vents (Guieu et al., 2018; Tilliette et al., 2022) as the buoyant hydrothermal plumes are able to reach surface waters (Zhang et al., 2020) providing the surface communities with an abundance of elements that can either be beneficial (Bonnet et al., 2023a) or detrimental to their physiology (Tilliette et al., 2023). The shallow hydrothermal vents in the WTSP release high concentrations of metals, including iron (Guieu et al., 2018; Tilliette et al., 2022; Wang et al., 2022); a lack of this critical micronutrient often limits marine productivity, particularly to nitrogen fixers in nitrogen-depleted waters, as they have a high iron requirement (Moore et al., 2013, 2001; Morel and Price, 2003). Iron inputs from shallow hydrothermal origin coupled with the >25°C sea surface temperature and phosphorus-rich waters of the WTSP (Bonnet et al., 2018; Caffin et al., 2018), had been hypothesized to lead to extensive blooms of diazotrophs, causing the area to be a global hotspot for nitrogen fixation (Bonnet et al., 2018, 2017; Shao et al., 2023). Recently, the link between shallow hydrothermal inputs, diazotroph blooms and enhanced carbon sequestration has been established in this region (Bonnet et al., 2023b).

It is important to understand the controls on bioactive metals in seawater, as they can profoundly affect biogeochemical cycles. Reduced sulfur substances (RSS) play an important role in trace metal complexation and thus on their availability, but little is known regarding their distribution in marine systems. RSS encompass a wide range of sulfur-containing molecules, including thiols, thioureas, thioamides and hydrogen sulfide. They can complex with metals, which can either inhibit metal toxicity or help with uptake (Dupont and Ahner, 2005; Huang et al., 2018; Mironov and Tsvelodub, 1996; Navarrete et al., 2019; Rea et al., 2004; Steffens, 1990; Walsh et al., 2015). Phytoplankton, plants and fungi have been shown to produce various RSS as a result of elevated metal exposure (Ahner et al., 2002; Bjørklund et al., 2019; Kumar et al., 2021; Pál et al., 2018). Leal and van den Berg (1998) showed that RSS can stabilise Cu as Cu^{+}, limiting concentrations of the more toxic Cu^{2+} (Leal and van den Berg, 1998). In environments with low trace metal concentrations, microbes have also been found to produce RSS to help with metal uptake (Huang et al., 2018; Walsh et al., 2015). RSS also act as antioxidants against reactive oxygen species (ROS) (Apel and Hirt, 2004; Madkour, 2020a, 2020b; Morris et al., 2022; Schieber and Chandel, 2014; Ulrich and Jakob, 2019). They are able to remove ROS by accepting their unpaired electron (McLeay et al., 2017; Morelli and Scarano, 2004), preventing tissue damage and injury (Baba and Bhatnagar, 2018; Dupont et al., 2004; Rijstenbil, 2002).

RSS can enter the marine environment through biological processes (Al-Farawati and van den Berg, 2001; Carfagna et al., 2016; Ciglenečki and Ćosović, 1996; Moran and Durham, 2019; Swarr et al., 2016), decomposition (Treude et al., 2009), sediments (Kiene, 1991; Kiene et al., 1990), cell leakage (Bluhm et al., 2010) and hydrothermal activity (McCollom and Seewald, 2007). They can be found throughout the marine environment, from estuaries to open ocean waters, and from the surface to the deep ocean. RSS can be removed from the marine environment through various sink processes. These include biological uptake by microorganisms (Moran and Durham, 2019) and photochemical processes (Chu et al., 2017; Laglera and van den Berg, 2006). In oxic seawater, RSS are typically present at nanomolar concentrations (Dupont et al., 2006; Gao and Guéguen, 2018; Swarr et al., 2016; Tang et al., 2000) while in anoxic environments, their concentrations can be much higher (Gomez-Saez et al., 2021; Mopper and Kieber, 1991); however, there are few studies focusing on their distributions and biogeochemical cycling.

Analytical detection and identification of RSS compounds in seawater, typically using chromatography or electrochemical techniques, is challenging due to the wide diversity of compounds and their relatively low concentrations (nM and below). Using high performance liquid chromatography (HPLC), only a few biogenic RSS compounds have been identified in seawater including glutathione, cysteine, γ-glutamate-cysteine and dipeptides such as arginine-cysteine or glutamine-cysteine (Dupont et al., 2006; Kawakami et al., 2006; Swarr et al., 2016). However, chromatograms also revealed the presence of a significant amount of other unidentified compounds, which are probably RSS (Swarr et al., 2016). Although powerful, the experimental methodology requires prior derivatization of the RSS before analysis and sometimes preconcentration, which may interfere with the integrity of the sample (Swarr et al., 2016).

Cathodic stripping voltammetry (CSV) at a mercury electrode is a simpler and faster technique, for detection of RSS. The method relies on the strong affinity between mercury and sulfur compounds, which causes an adsorbed complex to accumulate during the deposition step, followed by its reduction during the cathodic stripping scan. Although the reduction peak potential can be used to differentiate various sulfur compounds (Umiker et al., 2002), the peaks often coalesce when measured by CSV, resulting in a single, consolidated peak (Laglera et al., 2012). The detection of RSS has been carried out in both acidic and natural pH conditions. In acidic conditions (pH 2), two distinct peaks are attributed to RSS: one at -0.18 V and another at -0.09 V, corresponding to peak potentials for thioacetamide (TA) and glutathione (GSH), respectively (Pernet-Coudrier et al., 2013). Using this methodology in a recent study, we found that hydrothermal fluids can trigger the production of these RSS compounds by natural plankton communities (Tilliette et al., 2023). At natural pH, a single RSS peak is observed at ~ -0.52 V. Multiple RSS compounds such as glutathione, thiourea and thioacetamide produce peaks at similar potential (Whitby et al., 2018). Sulfide also produces a peak at this potential but it is unstable and tends to decrease rapidly (Al-Farawati and van den Berg, 1997). Table 1 presents a list of RSS compounds that

TABLE 1 Reduced sulfur species (RSS) detected in marine waters as well as common standards used for their quantification by voltammetry.

RSS	Location	Identification method	Approximate voltametric peak position*
Glutathione (GSH)	Subarctic Pacific Ocean	HPLC (Dupont et al., 2006) Detected to 500 m	Acidic (pH 2): -0.09 V (This study) Natural (pH 8.5): -0.51 V (This study)
	North Atlantic Ocean Sampled to 500 m	HPLC (Swarr et al., 2016) Detected to 500 m	
	Galveston Bay Surface water sampled	HPLC (Tang et al., 2000)	
Cysteine (Cys)	Subarctic Pacific Ocean	HPLC (Dupont et al., 2006) Detected to 500 m	Acidic (pH 1.95): -0.05 V (Pernet-Coudrier et al., 2013) Natural (pH 8.4): -0.40 V (Laglera et al., 2014) Natural (Cu(I)-Cys complex) (pH 8.5): -0.55 V (van den Berg et al., 1988)
	North Atlantic Ocean	HPLC (Swarr et al., 2016) Detected to 500 m	
γ-glutamyl-cysteine (γ-Glu-Cys)	Subarctic Pacific Ocean	HPLC (Dupont et al., 2006) Detected to 3000 m	Acidic: no data Natural: no data
Cysteinyl-arginine (Arg–Cys)	Subarctic Pacific Ocean	HPLC (Dupont et al., 2006) Detected to 500 m	Acidic (pH 1.95): -0.08 V (Pernet-Coudrier et al., 2013) Natural: no data
Cysteinyl-glutamine (Gln –Cys)	Subarctic Pacific Ocean	HPLC (Dupont et al., 2006) Detected to 500 m	Acidic: no data Natural: no data
Methanethiol (volatile)	Hydrothermal vent orifice	CSV (Dias et al., 2010)	Acidic (pH 2.3): -0.05 V (Dias et al., 2010) Natural (pH 8.15): -0.34 V (Whitby et al., 2018)
	Hydrothermal vent orifice	GC coupled with FID (Reeves et al., 2014)	
Sulfide	Hydrothermal system	Fluorescence (Radford-Knoery et al., 1998)	Acidic (pH 2): -0.18 V (This study) Natural (pH 8-8.1): -0.55 V (Al-Farawati and van den Berg, 1997)
Thioacetamide	Not naturally occurring in marine environments	CSV	Acidic (pH 2): -0.18 V (This study) Natural (pH 8.5): -0.54 V (This study) Acidic (Cu(I)-TA complex) (pH <1): -0.66 V (Jeng et al., 1990)
Thiourea	Not naturally occurring in marine environments	CSV	Acidic (pH 1.95): -0.23 V (Pernet-Coudrier et al., 2013) Natural (pH 8.4): -0.54 V (Laglera and Tovar-Sánchez, 2012)

*Peak positions are approximative because they are dependent on the chemical (e.g. pH, analyte concentration) and experimental (e.g. accumulation time, stripping parameters) conditions.

have been detected in marine waters along with their peak potential at the mercury electrode.

An alternative approach is cathodic pseudopolarography (CP). CP is a qualitative voltammetric technique (Laglera et al., 2014; Laglera and Tovar-Sánchez, 2012) that distinguishes between similar RSS compounds based on their potential-dependent adsorbing behaviour at the mercury surface. This technique consists of successive CSV measurements at varying deposition potentials (E_{dep}). By plotting the peak intensity vs E_{dep}, these pseudopolarograms may present waves that are characteristic of specific RSS compounds; the position and shape of these waves can be compared to those obtained from standards to help characterise the RSS present in the sample.

In this work, we use both CSV in acidic conditions and CP at natural pH to characterise the presence of RSS compounds throughout the water column and to identify their sources and sinks in the WTSP. This study was part of the French GEOTRACES TONGA project (shallow hydroThermal sOurces of trace elemeNts: potential impacts on biological productivity and the bioloGicAl carbon pump, GPpr14). We sampled from the mesotrophic Melanesian waters and North Fiji basin, through the hydrothermally active Lau Basin to the oligotrophic western south Pacific Gyre. We discuss the potential sources and sinks of RSS and we also compare pseudopolarograms of water column RSS to those of model standards (sulfide, GSH and TA) to further characterise these species.

2 Experimental

2.1 Sampling strategy

Samples were collected during the GEOTRACES TONGA (GPpr14) (Guieu and Bonnet, 2019) research cruise, which took place onboard the R/V L'Atalante from 31st October to 5th December 2019, a transect extending from New Caledonia to the western end of the South Pacific Gyre (Figure 1A).

Stations 2 and 3 were both in Melanesian waters in the western part of the transect. Station 2 was in the North Fiji Basin, north-west of the Hunter fracture zone while station 3 was situated in the South Fiji basin. Stations 4, 11 and 12 were in the Lau Basin in the central

10.3389/fmars.2024.1426906

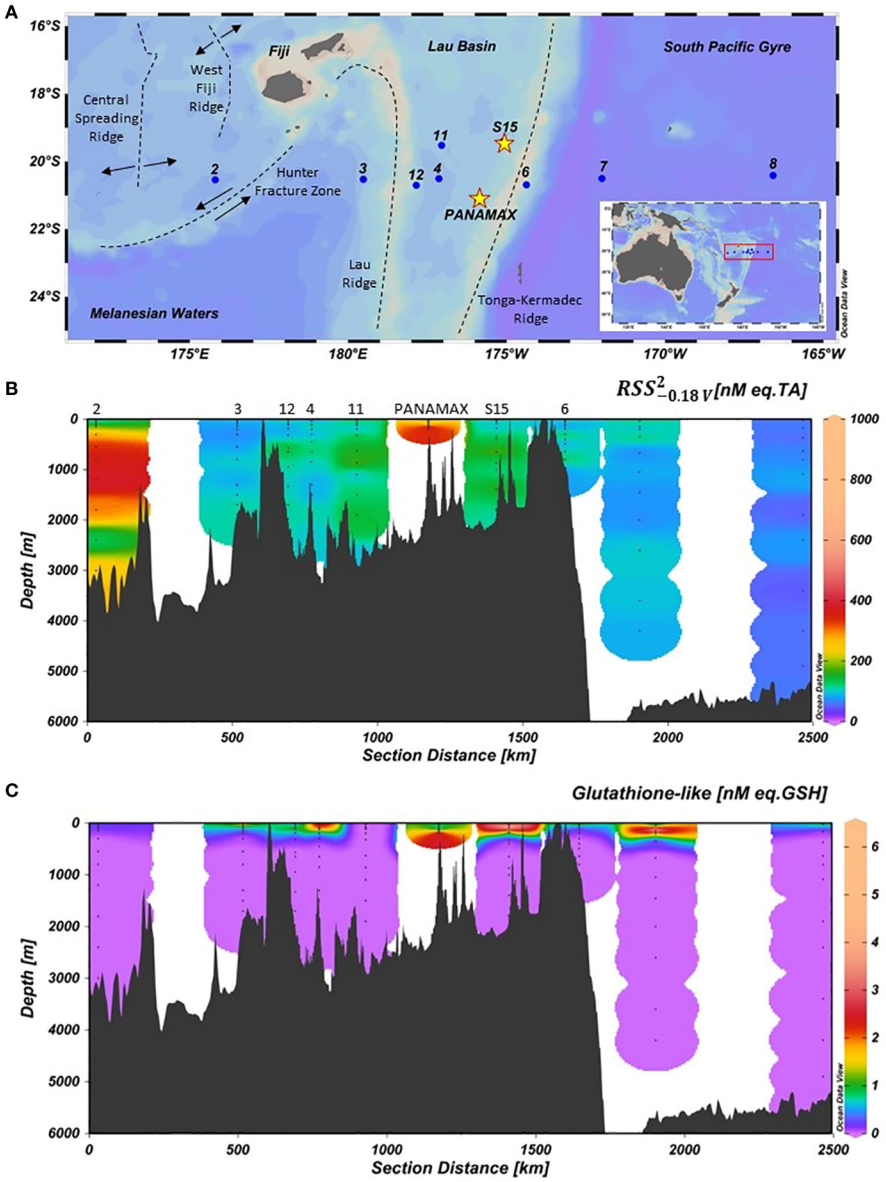

FIGURE 1
(A) Map of stations sampled during the TONGA 2019 cruise across the Western Tropical South Pacific Ocean (WTSP). In the WTSP there are three distinct regions: Melanesian waters, Lau Basin and South Pacific Gyre. The dashed lines represent plate boundaries. The numbers are the stations. The stars show the two shallow hydrothermal vents, PANAMAX and SIMONE. S15 was 15 km away from the SIMONE hydrothermal source but S15 still had high acoustic anomalies (Tilliette et al., 2022). **(B)** The distribution of $RSS^2_{-0.18\ V}$ compounds in nM eq. TA and **(C)** GSH-like compounds in nM eq. GSH. Figures were generated using ODV software (Schlitzer, 2021).

part of the transect while stations 6, 7 and 8 were in the South Pacific Gyre in the eastern part of the transect (Figure 1A). The transect also crossed two hydrothermal stations, PANAMAX and SIMONE, that were identified by acoustic anomalies (Bonnet et al., 2023a). At PANAMAX, strong and continuous anomalies of Eh, pH, redox potential and turbidity were detected, suggesting the presence of a hydrothermal plume. The sampling procedure followed at PANAMAX has been described elsewhere (Bonnet et al., 2023a). The SIMONE site also displayed multiple acoustic anomalies suggesting the presence of multiple weak hydrothermal sources (Tilliette et al., 2022). Four substations were sampled in the vicinity of SIMONE (T1, T2, T3 and T5) but only the furthest away (T1, 15 km away from hydrothermal vent) was analysed in this study. This station is referred as "S15".

2.2 Sample collection and storage

Samples were collected using a trace metal clean polyurethane powder-coated aluminium frame rosette (TMR, General Oceanics Inc. Model 1018 Intelligent Rosette), which was attached to a 6 mm diameter Kevlar line. The Go-Flo bottles were then transferred into a trace metal clean container (class 100) and pressurized with 0.2 µm-filtered nitrogen for sampling. Seawater was filtered through a

0.45 µm acid-cleaned polyethersulfone filter (Supor®) and collected in 125 mL Nalgene LDPE bottles, that had been acid-cleaned according to the GEOTRACES protocol (Cutter et al., 2017). Samples were collected after rinsing the bottle three times with around 20 mL of filtered sample, then double bagged and stored at −20°C until analysis.

2.3 Reagents

Water used for rinsing and dilution of reagents was ultrapure deionized water (>18 MΩ) from a Milli-Q (MQ) system (Millipore, UK). Thioacetamide (TA) (Fisher Scientific, UK) and glutathione (GSH) (reduced, Sigma-Aldrich, UK) were used as model RSS standards. Standards were acidified with HCl (laboratory reagent grade 32%, Fisher Scientific, UK) to pH 2. Hg plating solution was prepared from $Hg(NO_3)_2$ (Fluka, UK) in a 0.1 M sodium nitrate (Sigma-Aldrich, UK) and 10 mM HCl (Fisher, UK) solution. Stock solutions of 0.1 M sodium sulfide were prepared from hydrated $Na_2S.xH_2O$ (60-63%, Sigma-Aldrich, UK) on a daily basis. RSS standards were replaced when the concentration of the internal standard was no longer reproducible. All standards were kept in the dark to avoid photodegradation. When not in use, standards were kept in the fridge. For sulfide analysis, a borate buffer stock solution (1 M boric acid, reagent grade, Fisher Scientific, UK) was prepared in 0.35 M ammonia (trace metal grade, Fisher Scientific, UK), with the pH adjusted to 8.1. Organic contaminants were first removed from the buffer solution by UV-digestion; the solution was cleaned of trace metals by addition of 100 µM MnO_2 (van den Berg, 1982) and filtration using an acid cleaned 0.2 µm cellulose nitrate membrane (Whatman) after overnight equilibration.

2.4 Voltammetric equipment

For the quantifications of RSS and for the majority of CP, a µAutolabIII potentiostat (Ecohemie, Netherland) connected to a Metrohm 663 VA stand through the IME663 interface was used. A three-electrode cell consisted of a static mercury drop electrode (SMDE) as working electrode, a glassy carbon rod counter electrode and a Ag/AgCl//KCl (3 M) with glass salt bridge (Metrohm, filled with 3 M KCl) reference electrode. Connected to the VA stand was a V1 autosampler (https://sites.google.com/site/daromasoft/home/autosampler) allowing for the automatic loading and emptying of the voltammetric cell. Standard additions of TA and GSH standards were made automatically using Cavro syringe burettes. The voltammetric cell was rinsed twice with MQ for 30 seconds between each sample. Voltammetric analyses were controlled by NOVA software (version 2.1.4).

For CP of samples suspected to contain sulfide, a µAutolab potentiostat was connected to a Metrohm 663 VA stand through the IME663 interface and was controlled by the GPES software (Version 4.9) installed on a 32-bit laptop. A three-electrode system was also used. The working electrode was a 25 µm silver mercury amalgam microwire (silver microwire from Goodfellow, UK) fitted in a polypropylene pipette tip onto which a small vibrating rotor was fixed (1.5 V, 170 Hz) as described previously (Bi et al., 2013). Briefly, a Cu wire was inserted through a 100 µL pipette tip. The wire was connected to a 25 µm silver wire using a conductive, adhesive silver solution (Leitsilber L100, Maplin, UK). The Cu wire was pulled back leaving the silver microwire exposed out of the pipette tip. The tip was melted to secure the microwire by holding it in the mouth of a tubular oven set to 400 °C. The silver microwire was amalgamated with mercury by plating 2 mM Hg(II) (acidified at pH 2) at −0.4 V for 600 s in stagnant conditions. The amalgam electrode was then transferred to Milli-Q water and left overnight. The counter electrode was an iridium wire (approximately 2 cm in length, 150 µm diameter), and the reference electrode was an Ag/AgCl//KCl (3M) with a glass salt bridge filled with 3 M KCl.

2.5 Quantification of RSS concentrations

The voltammetric method used here was described by Pernet-Coudrier et al. (2013) to simultaneously quantify RSS and electroactive humic substances (referred to as refractory organic matter in the original paper). The concentrations and pseudopolarographic response of electroactive humic substances in these samples are reported elsewhere (Dulaquais et al., 2023; Portlock et al., in prep). Prior to analysis, 10 mL of seawater was acidified by adding 18µl of 1:1 MQ: HCL (reagent grade 32%) solution (final pH 2.04). Samples were also spiked with 100 nM molybdenum (Fisher scientific) for the determination of electroactive humic substances. Under a laminar flow hood, acidified seawater sample was automatically loaded into an acid-cleaned voltammetric quartz cell. Each new sample was purged with nitrogen (300s) before starting the analysis by CSV in differential pulse mode. The measurement consisted of a 30 s purge time, 150 s deposition at a potential (E_{dep}) of 0 V (with stirring on (setting 4 on the VA stand) followed by a 5 s rest (stirrer off) before the stripping scan (from 0 V to −0.6 V, modulation time of 60 ms, modulation amplitude of 60 mV, step potential of 2 mV and interval time of 0.1 s).

Similar to other studies (Fourrier and Dulaquais, 2024; Pernet-Coudrier et al., 2013), a well-defined peak was observed in all our acidified samples (pH 2) at a potential ~ −0.18 V, which was quantified using the standard thioacetamide (TA). Although the detected compound exhibits electrochemical characteristics similar to TA, TA is not naturally occurring in marine environments. Therefore, throughout the text, we refer to this peak in acidified conditions as a $RSS^2_{-0.18\ V}$ signal and give its concentration as TA equivalent. Similarly, in some samples, an additional broad peak was obtained at ~ −0.09 V. The $RSS^2_{-0.09\ V}$ signal exhibited a peak potential and shape similar to GSH; we refer to this peak as a GSH-like signal and we quantify its concentration in GSH equivalent. Quantification was done by standard additions (2 additions for each sample) of TA and GSH standards, added simultaneously. Typically, 4 repeat scans were performed for the analysis of the sample and after each of the 2 additions, giving a total of 12 scans for each determination and an approximate analysis time of 75 minutes per sample, including rinsing of the cell. In most cases, fixed standard additions of 80 nM TA and 1.6 nM GSH were made, unless the intensity of the initial peaks suggested a higher or lower concentration addition was required to quantify the peaks (see

Supplementary Figure S1 for example of voltammograms). For each measurement, the peak heights of $RSS^2_{-0.09\ V}$ and GSH-like signals were measured using ECDSOFT (Omanovic and Branica, 1998) after smoothing (Savitsky-Golay, smoothing factor 10).

Although TA is known to precipitate metals (Carrillo et al., 2018) and can form a Cu(I) complex in acidic conditions whose peak appear at -0.66 V (Table 1; Jeng et al., 1990) and interact with molybdenum (Farr and Laditan, 1974a and 1974b), all our standard additions were linear. This suggests that if complexation occurred, it had a negligible to impact the free TA concentration and/or the complexes are labile.

For quality control purposes, a Deep Sea Reference (DSR) seawater (Hansell lab, Batch 21 – 2021 – Lot 08-18, collected from 700m depth in the Florida Straits and acidified with HCl to pH 2) was used daily to check reproducibility. This was particularly important for TA because of instability in acidic conditions (Butler et al., 1958; Rosenthal and Taylor, 1957). The concentration of $RSS^2_{-0.18\ V}$ obtained in this reference seawater was measured at 56.1 ± 7.8 nM eq. TA (N=10, RSD =13.9%). If the daily check was not satisfactory, a new standard was made, which happened approximately on a monthly to bimonthly basis. Concentrations of GSH-like in the DSR were below the detection limits. The limit of detection was obtained by 3 times the standard deviation of 4 consecutive measurements of a seawater sample with low levels of TA (34 nM eq. TA) and GSH (2.5 nM eq. GSH). The limit of detection for TA was calculated to be 18 nM eq. TA and 0.43 nM for GSH. Error bars show the standard deviation of the intercept, determined by standard addition using Equation 1 (Harris, 2010).

$$s_x = \frac{s_y}{|\mathrm{m}|}\sqrt{\frac{1}{n}+\frac{\bar{\mathrm{y}}^2}{m^2\ \sum (x_i-\bar{\mathrm{x}})^2}} \quad (1)$$

Where s_x is the standard deviation of the compound being measured, s_y is the standard deviation in peak intensity across all data points, m is the slope of the standard addition, n is the number of data points (typically 12), $\bar{y}$ is the average peak height across all data points, x_i is the concentration of added standard for data points i, and $\bar{x}$ is the average concentration across all data points of the standard addition procedure.

2.6 Cathodic Pseudopolarography

CP was carried out on selected seawater samples, in unbuffered conditions (pH ~ 8.5), by recording the influence of the deposition potential on the intensity of the only RSS peak that we obtained at this pH (Supplementary Figure S1). This peak was located at ~ -0.52 V, similar to the peak reported in previous studies which is often attributed to the reduction of the Hg-S complex formed at the surface of the mercury during the accumulation step. In contrast to the quantification of $RSS^2_{-0.18\ V}$ and GSH-like signals, CP was achieved here only at natural pH because the peak is much more cathodic than the mercury oxidation wave (located in seawater at around -0.05 V), allowing for a wide range of deposition potentials to be tested. In acidic conditions, the $RSS^2_{-0.18\ V}$ and GSH-like peaks are present at relatively high potential thus limiting the range of deposition potential that could be tested.

For samples where the presence of sulfide was not expected, analysis was done on the SMDE in unbuffered, deoxygenated seawater samples. For comparison purposes, pseudopolarograms of TA and GSH standards (at 100 and 150 nM respectively) were obtained in UV digested seawater, also unbuffered and deoxygenated. For each pseudopolarographic experiment, 10 mL of seawater sample was loaded into an acid-cleaned voltammetric quartz cell and purged for 300 s. Pseudopolarograms started with an E_{dep} of 0 V and decreased by increments of -0.03 V until -0.72 V. The deposition time was 150 s at each E_{dep}, followed by a quiescence period of 5 s before the stripping scan (differential pulse from -0.3 V to -0.85 V, 20 ms modulation time, 60 mV modulation amplitude, 4 mV step potential 0.3 s interval time). Each pseudopolarogram took approximately 100 minutes to complete. Under these conditions of pH, only one natural RSS peak is detected at ~ -0.52 V and is referred here as $RSS^{8.5}_{-0.52\ V}$, much more cathodic than the 2 peaks obtained at pH 2 ($RSS^2_{-0.18\ V}$ and GSH-like), a change of approximately 55-63 mV/pH).

CP of samples suspected to contain sulfide were carried out using a Hg amalgam wire. Pseudopolarograms were obtained from an initial E_{dep} of -0.9 V up to 0 V, with +50 mV increment between successive measurements. The stripping parameters were as follows: differential pulse from -0.3 to -0.8 V, step of 6 mV, modulation amplitude of 50 mV, modulation time of 8 s and an interval time 0.1 s. The measurements were carried out without any purging nor stirring of the solution (instead the wire electrode was vibrated during the E_{dep}) to minimise the loss of sulfide during the experiment. A pseudopolarogram of the sulfide standard was obtained in 0.6 M NaCl (Fisher Scientific, UK) buffered at pH 9.2 with borate to minimise loss of sulfide through volatilisation (Aumond et al., 2012). The concentration of sulfide added was high (1 µM) allowing for a short deposition time (10 s). The sulfide peak potential was ~ -0.60 V, approximately 60 mV more cathodic than the TA peak (-0.54 V, Supplementary Table S1), even though these 2 peaks have been reported to have the same peak potential (e.g. Al-Farawati and van den Berg, 1997). The difference of 60 mV observed here can be attributed to differences in pH (9.2 vs 8.5, corresponding to around 40 mV cathodic shift) and differences in the working and reference electrodes. To account for these differences, the pseudopolarograms of all samples detected at the Hg amalgam wire were shifted anodically by 60 mV.

For comparison purposes, pseudpolarograms are given here as normalised to the highest intensity. Non-normalised pseudopolarograms of selected samples are given in Supplementary Figure S3.

3 Results

3.1 Hydrography and local conditions

A detailed account of the hydrography in this region has been previously described (Tilliette et al., 2022). Briefly, the Subtropical Underwater on the east and the Western South Pacific Central Water on the west dominated the main thermocline at a depth of 200 - 700 m, below the mixed layer (70 to 140 m). Immediately below were Antarctic Intermediate Waters, from 700-1300m, while the deep layer (> 1,300 m) composed two water masses: Pacific Deep Water (PDW)

and Lower Circumpolar Deep Water (LCDW). Across the cruise transect, the different water masses were distributed uniformly, except for the PDW and the LCDW. PDW was dominant in the Melanesian waters and Lau basin. In the Melanesian waters, LCDW was only present between 2,500 m and the seafloor. The Lau Basin had a low contribution of LCDW. However, in the deepest waters of the South Pacific Gyre, LCDW was the sole contributor.

Salinities ranged from 35.06 to 35.47 and temperature varied from 23.04 to 27.32 °C in the upper 100 m. The mixed layer ranged from 70-140 m deep during the cruise. The Lau basin is influenced by shallow hydrothermal activity, with at least two hydrothermal sites, PANAMAX and SIMONE (Figure 1A). Furthermore, a volcanic eruption in the region (Late'iki, previously Metis Shoal) began mid-October 2019, the month before the cruise. The main eruption continued until the 23rd October 2019 and minor eruptions continued into 2020. Satellite imagery suggested that there was a minor eruption on the 19th November (Yeo et al., 2022). S15 was the closest station in this study to Late'iki (~40 km south-west of Late'iki). S15 was sampled on the 24th November, 32 days after the main eruption ended and 5 days after the minor eruption.

3.2 Distribution of RSS in the WTSP Ocean

The distribution of $RSS^2_{-0.18\ V}$ and GSH-like compounds along the cruise transect are presented in Figures 1B, C respectively and the upper 500 m of all individual profiles are given in Figure 2. $RSS^2_{-0.18\ V}$ compounds were present throughout the whole water column at all stations, ranging from 48 to 984 nM (Figure 1B) with an average of 131 ± 16 nM across the transect (TA equivalent, N = 119). The average concentrations of $RSS^2_{-0.18\ V}$ compounds per station are given in Table 2. In the Lau Basin (stations 4, 11, 12, S15 and PANAMAX), the concentrations of $RSS^2_{-0.18\ V}$ compounds were higher than at adjacent stations (station 3 in the Melanesian waters and station 6 on the east side of the Tonga-Kermadec ridge). Moving further east to station 7 and 8 in the South Pacific Gyre, average TA concentrations decreased, with the lowest concentrations recorded at station 8. For most stations (3, 4, 6, 7, 8, 11 and 12), there were no clear trends with depth and the concentration remained quasi-uniform. The highest concentration (984 nM TA equivalent) was at PANAMAX (181 m). At the same depth, a strong decrease in Eh (Figure 2I) was observed (characteristic of reducing conditions), suggesting that the sample was collected in the hydrothermal plume. Station 2 (away from known hydrothermal activity) was characterised by high concentrations of $RSS^2_{-0.18\ V}$ compounds compared to the rest of the transect. At station 2, the average concentration of $RSS^2_{-0.18\ V}$ compounds were 242 ± 31 nM compared to the average concentration of 98 ± 12 nM across the cruise transect (excluding the PANAMAX station). $RSS^2_{-0.18\ V}$ concentrations at station 2 were similar to station 3 in the surface waters but were much higher at depth. While $RSS^2_{-0.18\ V}$ concentrations at station 3 remained between 66 and 112 nM throughout the water column, at station 2, there was a band of high $RSS^2_{-0.18\ V}$ material between 100 m and 3500 m, with a maximum concentration of 382 nM at 1200 m and high concentrations also in bottom waters, reaching 275 nM (Figure 1B). This pattern appears to be unrelated to water masses. GSH-like compounds were only detected in surface waters (upper 200 m) of most stations (Figure 1C). The concentrations ranged from 0.61 to 6.23 nM, with the maximum concentration observed at 46 m at station S15 in the Lau Basin (Figure 2D). Similar to $RSS^2_{-0.18\ V}$, GSH-like concentrations detected in the Lau Basin were slightly higher than those in adjacent waters (Table 2). At PANAMAX, concentrations of GSH-like compounds were also elevated (reaching almost 6 nM; Figure 2H) at the same depth as where the lowest Eh value was recorded suggesting that these samples were from the hydrothermal plume. In contrast to $RSS^2_{-0.18\ V}$, GSH-like concentrations detected at station 2 were relatively low, at similar levels as those encountered in the surface waters of station 7 and 8 of the oligotrophic South Pacific Gyre (Table 2). However, a high concentration (6.06 ± 0.9 nM) of GSH-like compounds was detected at 150m at station 7 (Figure 2D).

3.3 Pseudopolarography

3.3.1 Sulfide, glutathione and thioacetamide standards

Pseudopolarograms of sulfide, GSH and TA standards were recorded to be compared to those from selected samples at various stations. Although sulfide, GSH and TA all produce a peak located at a similar potential (at ~ -0.6, -0.51 and -0.50 V respectively), their pseudopolarographic response is different (Figure 3): sulfide can be detected at E_{dep} > -0.65 V (wave at around -0.63 V), GSH at E_{dep} > -0.5 V (wave around -0.45 V) while TA is only detected at E_{dep} > -0.075 V (wave around -0.04 V, Figure 3). The potential at which the pseudopolarographic waves occur is dependent on the stability of the adsorbed complex at the mercury surface. In the case of sulfide, mercury is easily oxidised due to the formation of the highly insoluble HgS complex pushing the reduction wave towards negative values. For GSH and TA, the waves are more positive and well separated. While GSH and TA are stable compounds during the experimental time (same pseudopolarograpms were obtained when repeated in the same solution), sulfide is well-known for its instability and rapid loss of signal, preventing analysis using the SMDE (Al-Farawati and van den Berg, 1997). Instead, we recorded the pseudopolarogram of sulfide under conditions that minimise its loss (see experimental section). Sulfide can be detected without any interference from GSH and TA when using a E_{dep} of -0.6 V. When E_{dep} is increased above that value, the sulfide signal intensity tends to decrease which is likely due to some loss of sulfide from solution, either through volatilisation, oxidation or complexation.

3.3.2 Marine samples

Surface, mid-water depth and bottom water samples from hydrothermal stations in the Lau Basin and from station 8 (the most representative open ocean sample), were analysed by CP to determine whether $RSS^{8.5}_{-0.52\ V}$ changed with depth and between both biogeochemical provinces. In addition, one sample from mid-depth at station 2, where high $RSS^2_{-0.18\ V}$ concentrations were detected, was chosen at random for characterisation of these RSS.

3.3.2.1 The Lau basin

Pseudopolarograms were performed on samples collected at PANAMAX (25, 110, 181 m) and at S15 (19, 399 and 1780 m

10.3389/fmars.2024.1426906

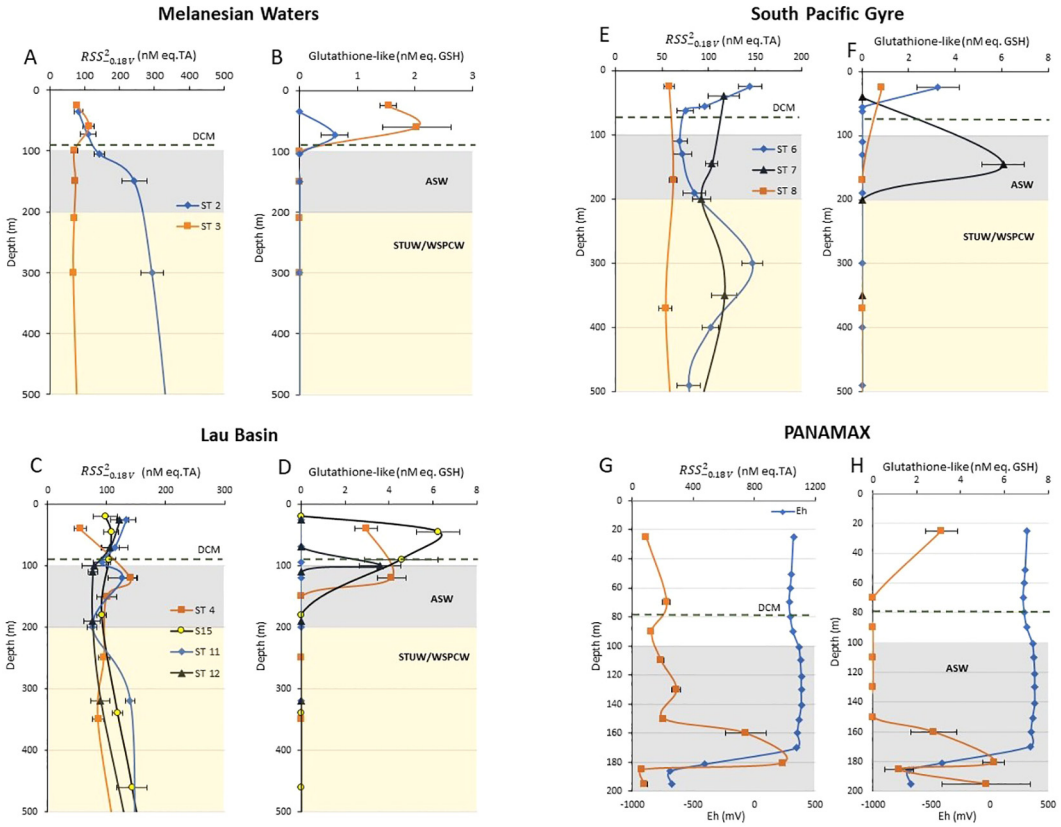

FIGURE 2
Concentrations of $RSS^2_{-0.18\ V}$ compounds in nM eq. TA and GSH-like compounds in nM eq. GSH in the upper 500 m of the Melanesian Basin **(A, B)**, Lau Basin **(C, D)** and South Pacific Gyre **(E, F)**. S15 was 15 km away from the SIMONE hydrothermal source. The shallow hydrothermal vent PANAMAX **(G, H)** was plotted separately along with Eh. Dashed line represents the average deep chlorophyll max (DCM) in each oceanographic region. There is no FluoChl data for stations 7 and 8, as the fluorimeter was unmounted at these stations. Concentrations were obtained using standard additions. Colour blocks show the different water masses. Artifactual Surface Water (ASW), Subtropical Underwater (STUW) and Western South Pacific Central Water (WSPCW) (Tilliette et al., 2022). Each of the profiles from each oceanographic region was plotted over 0–500 m **(A–F)**, except for PANAMAX which is plotted over 0–200 m **(G, H)**. Note that the scale of the x axis differs.

TABLE 2 Average concentration of $RSS^2_{-0.18\ V}$ and GSH-like compounds at each station. $RSS^2_{-0.18\ V}$ compounds were detected throughout the entire whole water column. GSH-like compounds were detected only detected in the upper 200 m.

Location	Station	Average $RSS^2_{-0.18\ V}$ compounds (nM eq.TA)	Average GSH-like concentration (nM eq.GSH)
Melanesian waters	2	242 ± 31	0.61 ± 0.23
	3	87 ± 7	1.76 ± 0.37
Lau Basin	4	99 ± 16	3.54 ± 0.57
	S15	122 ± 17	5.40 ± 1.34
	11	121 ± 18	<LOD
	12	104 ± 14	3.6 ± 0.95
	PANAMAX	285 ± 27	3.56 ± 0.99
South Pacific Gyre	6	98 ± 10	3.26 ± 0.91
	7	91 ± 10	6.06 ± 0.9
	8	61 ± 6	0.83 ± 0.13

<LOD, below detection limit.

depth). One sample of particular interest was the deep sample at PANAMAX (depth of 181 m), collected within the hydrothermal plume. As sulfide was likely present in this sample, pseudopolarograms were obtained at both the SMDE and Hg-Ag wire electrode (Figure 4). Firstly, the response of the sample at the Hg-Ag wire is very similar to that of the sulfide standard, highlighting the presence of sulfide. The concentration in the voltammetric cell was estimated to be >225 nM (estimation made from sensitivity obtained with 1 µM sulfide at E_{dep} = -0.59 V). Secondly, the response obtained at the SMDE following purging (assuming a complete loss of sulfide) with the peak height increasing with increasing E_{dep} suggests the presence of several RSS compounds: the lowest reduction wave detected at around -0.44 V was similar to GSH (reduction wave around -0.45 V). However, comparison with the pseudopolarogram of the TA standard strongly suggests that TA is not present at any significant concentration in this sample, if at all. The pseudopolarogram of the plume sample obtained at the SMDE did not experience sulfide interference as the sample was purged prior to analysis.

The other five samples tested from the Lau Basin (from 25 and 110m at PANAMAX and 19, 399 and 1780 m at S15) displayed pseudopolarograms with a very similar pattern (Figure 5), all having

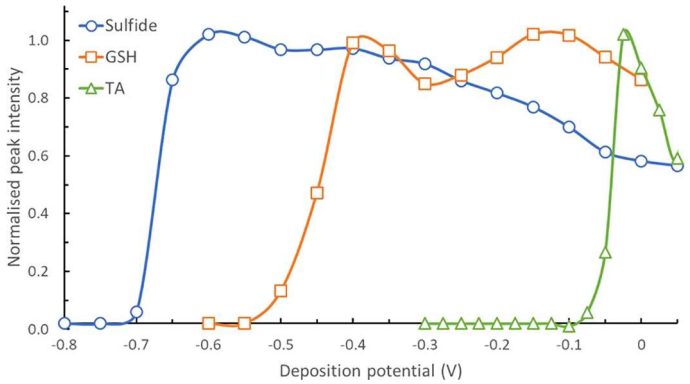

FIGURE 3
Normalised pseudopolarograms of sulfide, GSH and TA obtained (using SMDE at pH 8.5 see conditions in experimental section). For comparison purposes, pseudopolarograms are displayed as normalised to their highest peak intensity. In each case, the RSS peak being monitored is located at around -0.52 V (see Supplementary Table S1). Note that the sulfide data was obtained at a pH of 9.2 at the Hg-Ag wire and has been normalised to a pH of 8.5 at the HMDE by shifting the potential anodically by 60 mV. Peak potentials are in Supplementary Table S1.

a relatively positive reduction wave (from -0.15 to -0.05 V) irrespective of depth, indicating that GSH is not present in those samples. This is in agreement with results obtained in acidic conditions where GSH-like compounds were below detection limits for the PANAMAX 110 m sample and S15 19 m, 339 m and 1780 m samples (Figure 2). However, for the surface sample at PANAMAX (25 m), GSH-like compounds were found in acidic conditions but the pseudopolarogram did not display any reduction wave similar to that of GSH standard.

3.3.2.2 Station 8 – South Pacific Gyre

Pseudopolarograms of $RSS^{8.5}_{-0.52\ V}$ at station 8 (at depths of 25, 2400 and 5462 m) are shown in Figure 6. In contrast to other non-hydrothermal stations, the pseudopolarograms at station 8, particularly at 25m, extend much further cathodically: in the sub-surface sample, a reduction wave at around -0.47 V was observed, similar to the sample within the hydrothermal plume at PANAMAX after sulfide removal (obtained at the SMDE, Figure 4), both of which occurred at a similar potential as the reduction wave obtained for GSH. A second wave at ~ -0.15 V was also observed together with a slight increase at 0 V, similar to that of the TA. As depth increased (depth 2400 m), this most cathodic wave decreased in intensity and shifted slightly anodically (to ~ -0.44 V), still similar to GSH but no GSH-like signal was detected in acidic conditions. The signal intensity increased strongly and almost continuously at E_{dep} > -0.1 V highlighting the presence of unidentified compounds. In the deep sample (5462 m), a signal was only obtained for E_{dep} > -0.2 V with the presence of a wave at -0.15 V and -0.05 V, similar to that of TA standard.

3.3.2.3 Station 2 – North Fiji Basin

Figure 7 presents the pseudopolarogram of $RSS^{8.5}_{-0.52\ V}$ in a sample from station 2 where the TA concentration was particularly high ([TA] = 367 ± 33 nM, depth of 797 m,

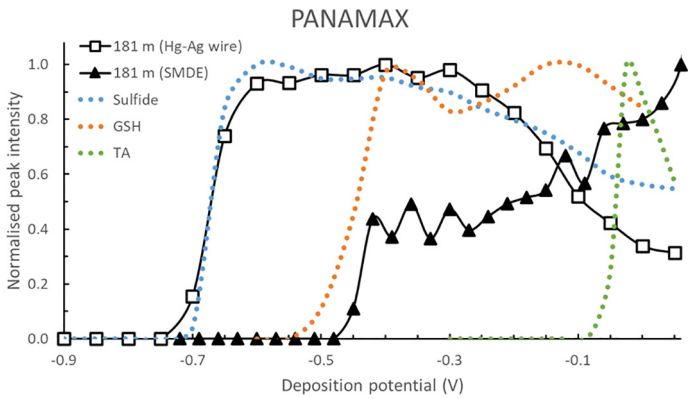

FIGURE 4
Normalised pseudopolarograms $RSS^{8.5}_{-0.52\ V}$ of the PANAMAX sample collected at 181 m (within the hydrothermal plume) using the Hg-Ag wire (15 s deposition time, for detection of sulfide) and using the SMDE (150 s deposition time for detection of other RSS). For comparison purposes, the response of the sulfide (most cathodic wave), GSH (middle wave) and TA (most anodic wave) standards are shown in dotted lines. The arrows represent the direction that the Edep was varied: anodic for the wire (sample and sulfide standard) and cathodic at the SMDE (sample, GSH and TA standards). In each case, the RSS peak being monitored is located at around -0.52 V (see Supplementary Table S1). Note that the sulfide data was obtained at a pH of 9.2 at the Hg-Ag wire and has been normalised to a pH of 8.5 at the SMDE by shifting the potential anodically by 60 mV. Peak potentials are in Supplementary Table S1.

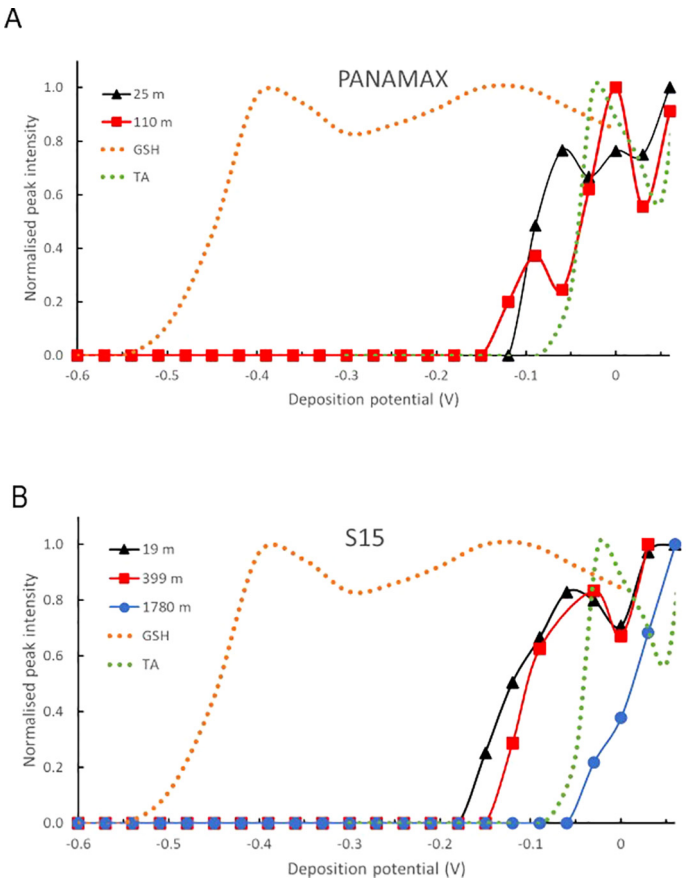

FIGURE 5
Normalised pseudopolarograms of $RSS^{8.5}_{-0.52\ V}$ in samples collected in the Lau Basin at various depths **(A)** at PANAMAX (25 and 110 m) and **(B)** at S15 (19, 399 and 1780 m). Pseudopolarograms obtained using the SMDE electrode, 150s deposition time. For comparison purposes, the response of the GSH (most cathodic wave) and TA (most anodic wave) standards are shown in dotted lines. In each case, the RSS peak being monitored is located at around -0.52 V (see Supplementary Table S1). Peak potentials are in Supplementary Table S1.

Figure 1B). A reduction wave at around -0.58 V was observed, ~ 50 mV more anodic than that of sulfide and 130 mV more cathodic than GSH. The peak intensity increased when increasing the E_{dep}, with two faint reduction waves seen at -0.32 V and -0.13 V, highlighting the presence of other unidentified RSS compounds. The expected increase at high E_{dep} observed with the TA standard was not seen in this seawater sample, showing that TA is not present in significant concentrations in this sample.

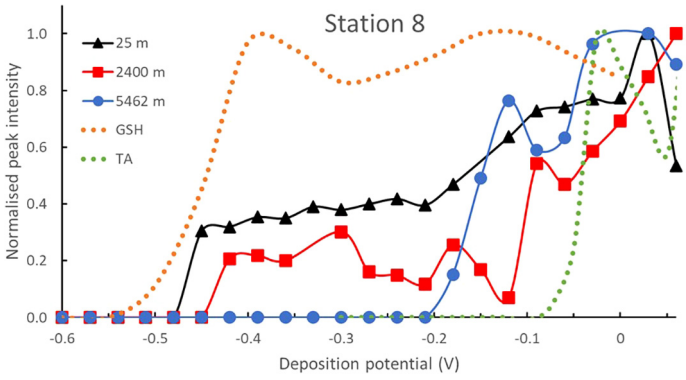

FIGURE 6
Normalised pseudopolarograms of $RSS^{8.5}_{-0.52\ V}$ in samples collected in the oligotrophic South Pacific Gyre, at Station 8 (25, 2400 and 5462 m). Pseudopolarograms obtained using the SMDE electrode, 150s deposition time. For comparison purposes, the response of the GSH (most cathodic wave) and TA standards (most anodic wave) are shown in dotted lines. In each case, the RSS peak being monitored is located at around -0.52 V (see Supplementary Table S1). Peak potentials are in Supplementary Table S1.

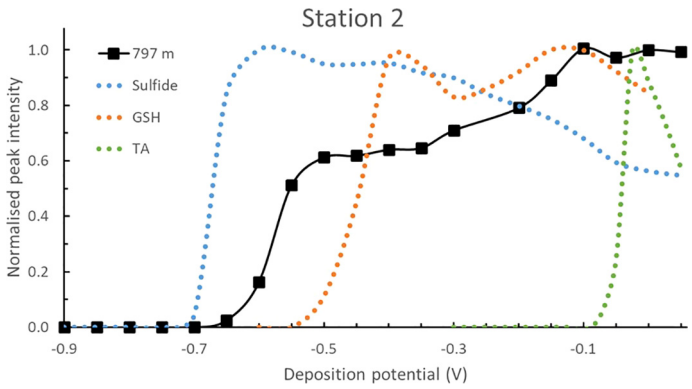

FIGURE 7
Normalised pseudopolarograms of $RSS^{8.5}_{-0.52\ V}$ in the sample collected at station 2, 797 m depth using the Hg-Ag wire (90 sec deposition time). For comparison purposes, the response of the sulfide (most cathodic wave), GSH (middle wave) and TA (most anodic wave) standards are shown in dotted lines. Peak potentials are in Supplementary Table S1. The peak potentials of the peaks being monitored in each pseudopolarograms are given in Supplementary Table S1. Note that both the sulfide and the 797 m sample data was obtained at a pH of 9.2 at the Hg-Ag wire. They have been normalised to a pH of 8.5 at the SMDE by shifting the pseudopolarogram anodically by 60 mV. Peak potentials are in Supplementary Table S1.

4 Discussion

4.1 RSS distribution in the WTSP

The vertical profiles of $RSS^2_{-0.18\ V}$ and GSH-like compounds suggest a combination of distinct and common processes drive their biogeochemical cycling. Both show some evidence of photodegradation, with near surface samples typically having a lower concentration than in underlying waters. For GSH-like compounds, this was seen at most stations, whereas for $RSS^2_{-0.18\ V}$ compounds, this was only observed at stations 2, 3 and 4. Photochemical destruction of RSS has been demonstrated to occur on the order of hours (Gomez-Saez et al., 2017; Laglera and van den Berg, 2006; Moingt et al., 2010). In the presence of UV-light, TA was reported to photodegrade at a faster rate than GSH (Laglera and van den Berg, 2006). In this study, $RSS^2_{-0.18\ V}$ compounds showed less evidence of photodegradation compared to GSH-like compounds, suggesting that active production of $RSS^2_{-0.18\ V}$ compounds is higher, or at the same rate of the photodegradation, or that the $RSS^2_{-0.18\ V}$ compounds do not behave identically to TA. Complexation with metals can affect photodegradation of RSS. Cu complexation has been shown to extend the half-life of TA, whereas it has been shown to accelerate the oxidation of GSH (Laglera and van den Berg, 2006; Moingt et al., 2010). The ratio of RSS to Cu determines how Cu complexation affects RSS photodegradation. In the surface waters (upper 200 m) of TONGA, the average concentration of total dCu was ~ 0.4 nmol kg^{-1} (Gonzalez-Santana., pers. comms. March 2024), which is relatively low compared to the RSS concentrations obtained in this study, suggesting that Cu complexation do not play a substantial role in RSS photodegradation.

Marine microbes have been shown to produce RSS both intracellularly and extracellularly when exposed to light in order to reduce stress from ROS (Mangal et al., 2020; Sunda et al., 2002). Previous studies have found a correlation between RSS, particularly GSH-like, with Chl *a* (Al-Farawati and van den Berg, 2001; Hu et al., 2006). In November 2019 in the WTSP, marine microbes were exposed to sunlight for ~ 13 h per day, which may have stimulated the production of RSS.

GSH-like compounds were only detected in the upper 200 m, suggesting biological production in surface waters, at concentrations similar to previous studies using a range of methods (Dupont et al., 2006; Kading, 2013; Le Gall and van den Berg, 1998; Swarr et al., 2016; Whitby et al., 2018). In this study, we found no correlation between the distribution of GSH-like compounds with Chl *a* (data not shown). For the majority of stations, a GSH-like maxima were observed sub-surface but above the deep chlorophyll max. Heterotrophic bacteria have also been suggested as a source of GSH-like compounds, which may explain the lack of correlation between GSH-like compounds and Chl *a* observed here, consistent with previous studies (Cameron and Pakrasi, 2011; Carfagna et al., 2016; Swarr et al., 2016). While heterotrophic bacteria are more abundant in the photic layer (0-100 m), unlike phototrophs, heterotrophic bacteria are present throughout the water column, therefore GSH-like compounds would be expected throughout the water column. However, GSH-like compounds were confined to the surface, possibly indicating low abundance and/or low metabolic activity of heterotrophs at depth. GSH-like compounds may still be produced at depth, but their turnover rate may be slower than their oxidation rate, which is only a few hours (Petzold and Sadler, 2008). The highest surface GSH concentration was detected at station S15 (6.23 nM at 46 m) in the hydrothermally active Lau Basin, possibly following the Late'iki eruption.

In comparison, $RSS^2_{-0.18\ V}$ compounds were detected at all depths across the transect (Figure 1B). $RSS^2_{-0.18\ V}$ compounds did not experience the same sub-surface maxima as GSH-like compounds, and there was no correlation between the distribution of $RSS^2_{-0.18\ V}$ compounds and Chl *a* (data not shown). However, this does not mean that $RSS^2_{-0.18\ V}$ compounds are not of biological origin. A previous study found that phytoplankton actively exude a compound electrochemically similar to TA (Leal et al., 1999). The lack of

correlation could be due to the stability of $RSS^2_{-0.18\ V}$ compounds away from direct sunlight, similar to TA which is relatively stable for long periods depending on environmental conditions (Howard et al., 2017; Mallory, 1968) allowing for its accumulation throughout the water column. TA can be a source of sulfur for marine microbes (Schmidt et al., 1982) which might also be the case for $RSS^2_{-0.18\ V}$. The persistence of $RSS^2_{-0.18\ V}$ compounds with depth could suggest that their uptake is slower than their rate of production.

We found slightly higher average concentration of GSH-like compounds than in previous studies, with a mean concentration of 3.4 ± 0.8 nM across the transect, compared to maximum concentrations of 0.8, 1.7 and 2.2 nM GSH in studies by Dupont et al. (2006); Kading (2013) and Swarr et al. (2016) respectively. The concentrations of $RSS^2_{-0.18\ V}$ compounds were lower than those detected in the North Pacific (Fourrier and Dulaquais, 2024) where they ranged from 118 ± 14 to 1140 ± 137 nM, with concentrations decreasing from surface to deep water. These nanomolar concentrations levels are much higher than those detected at natural pH in the North East Pacific where sub nM concentrations of RSS compounds were reported (Whitby et al., 2018). This large difference has to come from different experimental conditions (pH, standard, deposition potential) and different behaviour to these changes between the natural compounds and the standard. For instance, in our experiments, the intensity of the peaks at natural pH and in acidic conditions are in the same order of magnitude (nA range) while the sensitivity of the TA sharply decreases from natural pH to acidic conditions by a factor of at least 200 times. Although the reason for this loss in sensitivity is unclear (it cannot be explained by the protonation of TA in acidic conditions (pK of 1.76, (Rosenthal and Taylor, 1957)), this difference between the natural peak and the TA standard provides further evidence that the RSS peak at natural pH ($RSS^{8.5}_{-0.52\ V}$) is certainly not TA. Consequently, the concentration values reported here are conditional to the experimental parameters, are not relevant to TA and should therefore only be compared with great care to concentrations obtained by other techniques (or other pH).

Concentrations of both $RSS^2_{-0.18\ V}$ compounds and GSH-like compounds at the surface were higher in the Lau Basin than in the adjacent Melanesian Basin and South Pacific Gyre (Table 2), with concentrations decreasing with distance away from the Lau Basin. The Lau Basin experiences high primary production and high diazotrophic activity due to extensive shallow hydrothermal activity (Bonnet et al., 2023b) which might explain the higher levels of $RSS^2_{-0.18\ V}$ and GSH-like compounds. Hydrothermal vents also release trace metals such as copper, nickel, zinc and lead which can all be toxic to marine microbes, triggering biological production of RSS to reduce metal toxicity (Bjørklund et al., 2019; Courbot et al., 2004; Dupont and Ahner, 2005; Huang et al., 2018; Kumar et al., 2021; Navarrete et al., 2019; Pál et al., 2018; Steffens, 1990; Vasconcelos and Leal, 2001). In sulfidic conditions, high RSS concentrations (>500 nM) have been measured, such as in the Black Sea (Mopper and Kieber, 1991) and in sediment pore waters (Chapman et al., 2009). While such high concentrations were not observed here, the nearby volcanic and hydrothermal activity could also contribute to higher RSS concentrations.

The concentrations of $RSS^2_{-0.18\ V}$ compounds in the South Pacific Gyre decreased with distance away from the Lau Basin, suggesting an apparent dilution or weakening of the process responsible for its production in the Lau Basin, similar to what was previously observed for iron-binding ligands and DOM more broadly in this region (Mahieu et al., 2024). Station 8 displayed the lowest concentration of TA (average of 62 ± 5 nM in acidic conditions). In contrast, electroactive humic substances, which can also act as organic metal-binding ligands, were elevated at this station relative to other stations (Dulaquais et al., 2023; Portlock et al., in prep.).

4.2 Hydrothermal influence on sulfide and RSS production

In the PANAMAX plume (181 m), elevated concentrations of $RSS^2_{-0.18\ V}$ (984 ± 19 nM; Figure 2G) and GSH-like compounds (5.5 ± 0.5 nM; Figure 2H) were detected along with the presence of sulfide (>225 nM), suggesting active production of these compounds related to hydrothermal activity, either through abiotic or biotic processes. While µM levels of methanethiol have been detected in hydrothermal fluids (Dias et al., 2010; Reeves et al., 2014), no voltammetric signal was observed at its expected potential (Table 1; acidic pH -0.09 V; natural pH -0.43 V), probably because of dilution of the plume as well as a known short residence time for CH_3SH (Schäfer and Eyice, 2019).

Abiotic production of RSS in hydrothermal systems is tied to the thermodynamic and geochemical constraints of the system (temperature, pressure and chemical elements/starting materials). PANAMAX was characterised as having low O_2 concentrations (<150 µM), high CH_4 (>104 nM), high CO_2 (>645 µM), relatively high Fe (>50 nM) (Tilliette et al., 2022) and high H_2S (estimated at >225 nM, this study). The temperature and pH of the end-member fluids released from PANAMAX were not measured in this study, but the plume was recorded to be 21.2°C (mean of rest of transect (~200 m) 20.8°C) and the pH was found to be around 6.5 (Tilliette et al., 2023). The temperature of the fluids released from PANAMAX can be estimated from seawater boiling curves (Hannington et al., 2005; Stoffers et al., 2006). As PANAMAX is at a depth of around 200 m, it would imply that the temperature of end-member fluid would be no higher than 200°C. Although the pH of the end-member fluid is not known, other hydrothermal vents in the TONGA region have been reported to range from pH 1.2 to 6.1 (Hsu-Kim et al., 2008; Peters et al., 2021; Stoffers et al., 2006). The abiotic production of methanethiol can occur from the reaction of H_2S with hydrogen and CO/CO_2 (at 25°C and 1 bar) and theoretical calculations indicate that this reaction is viable in hydrothermal systems (Schulte and Rogers, 2004). CO was not measured in this study and has not been reported in hydrothermal systems, but experimental studies indicated that CO and CO_2 equilibrate at temperatures of ≥150°C (Foustoukos et al., 2001; Schulte and Rogers, 2004). Methanethiol can be a precursor for other RSS. Another chemical pathway is the reaction of H_2S, CO_2 and iron sulfide (FeS), a common component of hydrothermal systems (Findlay et al., 2019; Yücel et al., 2011), under anaerobic conditions, which yields a wide variety of organic sulfur compounds, mainly RSS, the production rate being largely influenced by the temperature (Heinen and Lauwers, 1996).

The production of RSS could also be due to biotic processes. Hydrothermal vents are able to sustain a wide variety of organisms due to the release of high concentrations of both metals and non-metals (Klinhammer et al., 1977; Resing et al., 2015), which can act as bio-essential nutrients for marine microbes (Aparicio-González et al., 2012; Lohan and Tagliabue, 2018). However, elevated concentrations of some chemicals can be harmful to marine microbes. In addition to the native biology around hydrothermal vents, buoyant hydrothermal plumes of the shallow vents (<200 m) can also reach the surface waters, affecting biological activity and RSS production. A recent study by Tilliette et al., 2023, found that when surface communities collected during the cruise in TONGA were exposed to hydrothermal fluids from PANAMAX, there was production of $RSS^{2}_{-0.18\ V}$ and GSH-like compounds (referred to as TA-like and GSH-like compounds). The addition of hydrothermal fluids led to the immediate production of $RSS^{2}_{-0.18\ V}$ compounds, thought to be produced by Synechococcus ecotypes to detoxify their environment. In contrast, GSH-like compounds were produced gradually over time, suggesting that they were not produced to detoxify the environment. Marine microbes have been found to produce GSH-like compounds to disassociate strongly bound Cu and act as a 'weak ligand shuttle', to make Cu accessible (Semeniuk et al., 2015). The use of GSH-like compounds as a 'weak ligand shuttle' may not be limited to Cu.

GSH also plays a vital role in the growth and regulation of marine microbes and therefore is abundant intracellularly (Ahner et al., 2002; Dupont et al., 2004; Giovanelli, 1987). The elevated concentrations of GSH-like compounds at PANAMAX could also be due to the breakdown of cyanobacteria. In the study by Tilliette et al., 2023, the abundance of cyanobacteria decreased after the addition of PANAMAX hydrothermal fluids, possibly due to addition of metal rich fluids. Cyanobacteria are extremely sensitive to dCu (Brand et al., 1986). Concentrations of dCu within the PANAMAX plume were similar to the rest of the transect (hydrothermal plume 0.4 nmol kg^{-1}; Gonzalez-Santana., pers. comms. March 2024), however Cu toxicity depends on its speciation. In some hydrothermal systems, dCu concentrations have been found to exceed ligand concentrations (Kleint et al., 2015), which could increase Cu toxicity and stimluate the production of GSH or the release of intracellular GSH-like compounds into the marine environment from cellular breakdown.

Hydrothermal vents are well-known to be a source of sulfides (Cotte et al., 2018; Damm et al., 1995; Dias et al., 2010), including those from the Lau Basin (Hsu-Kim et al., 2008; Yücel et al., 2011). Here, sulfide was identified only in the sample collected in the plume (Figure 4), with an estimated concentration > 225 nM. In this sample, a reduction wave at -0.44 V was apparent at the SMDE, similar to GSH-like compounds, and in agreement with the signal detected in acidic conditions (quantified as 5.5 nM). The signal increased with increasing E_{dep} highlighting the presence of other, unidentified RSS compounds in the plume. Although the PANAMAX vent is shallow at around 200 m, pseudopolarograms of $RSS^{8.5}_{-0.52\ V}$ in samples collected at the sub-surface (25 m) and below the deep chlorophyll max (110 m) did not show reduction waves characteristic of sulfide or GSH standards (Figure 5A), suggesting that RSS present in the plume at 180 m depth are not sufficiently stable to reach surface waters.

4.3 Station 2 – North Fiji Basin

$RSS^{2}_{-0.18\ V}$ concentrations were high throughout the water column at station 2 compared to the rest of the transect. Meanwhile, GSH-like were only detected in surface waters (Figure 1C). High concentrations of Fe-binding ligands were also found at depth at station 2 (max concentration at 1800 m, see Mahieu et al., 2024). The presence of high RSS and Fe-binding ligands at this station suggests either the production of these compounds within the water column or input from hydrothermal systems. Station 2 is located in the North Fiji Basin, which is a highly complex back arc-basin. To our knowledge, the North Fiji Basin has two spreading ridges (Central spreading ridge and West Fiji Ridge, Figure 1), as well as multiple fracture zones. Other oceanographic regions with multiple plate boundaries experience intense hydrothermal activity. Active venting has been confirmed in the North Fiji basin (Bendel et al., 1993), along with evidence of a 'megaplume' (Nojiri et al., 1989). Megaplumes have also been observed in the neighbouring Lau Basin (Baumberger et al., 2020). Megaplumes or event plumes are a significant, intermittent release of hydrothermal activity. These eruptions produce a buoyant plume that can be observed up to 1000 m above the sea floor. Previous megaplumes have been found to be 20 km in diameter and have a thickness of 700 m (Baker et al., 1987), which could explain why we observe high concentrations of $RSS^{2}_{-0.18\ V}$ compounds, at depth. While no active vents have yet been reported near station 2, their existence cannot be ruled out definitively. These areas are rarely investigated as most studies focus on the plate boundaries.

High metal concentrations are typically evidence for the presence of hydrothermal vents, however this is not the case at station 2. Dissolved Fe concentrations increased from 1000 m to the seafloor (above 0.5 nmol kg^{-1}) but this increase was not significant compared to the rest of the transect (Tilliette et al., 2022). Other dissolved metals such as Cu and Zn did not show an increase compared to the rest of the transect (Gonzalez-Santana, pers. comms. March 2024). Hydrothermal vent fluid chemistry is linked to the conditions which the vent is situated in and may release metal concentrations similar to seawater (Hodgkinson et al., 2015; Seyfried et al., 2015). These low metal vents have been found in ultramafic rocks, where metals in the fluids precipitate out in sub surface reactions. Dredges from the Hunter Fracture Zone have a large amount of ultramafic rock (Tararin et al., 2003). In addition, hydrothermal vents hosted in ultramafic rock are thought to produce ideal conditions for the production of organic compounds (Konn et al., 2009; Lang et al., 2010; Sander and Koschinsky, 2011).

At the time of the cruise, station 2 was on the convergence of two counter-rotating eddies, which saw high abundance of *Trichodesmium* compared to the surrounding areas (Benavides et al., 2021). Over time these communities sink. While N_2 fixation rates decrease with depth, *Trichodesmium* and other diazotrophs are still active in the mesopelagic zone (Benavides et al., 2022). For some diazotrophic bacteria there is a link between N_2-fixation and RSS biosynthesis. Diazotrophs are able to produce RSS to complex with ROS generated during N_2-fixation (Bocian-Ostrzycka et al., 2017). It is also thought that RSS play a role in N_2-fixation,

potentially as cofactors for enzymes involved in N_2-fixation or as signalling molecules that regulate the activity of genes related to N-fixation (Kalloniati et al., 2015). This link of N_2-fixation and RSS biosynthesis is primarily linked to terrestrial diazotrophs and should be investigated for marine diazotrophs. As diazotrophs sink and experience stress/death, they may release intracellular RSS, which may have contributed to the elevated concentrations of $RSS^{2}_{-0.18\ V}$ compounds at this station.

4.4 RSS diversity in the WTSP

RSS encompass a wide range of sulfur-bearing compounds and pseudopolarography is helpful to differentiate compounds (e.g. Figure 3). For instance, when comparing the pseudopolarograms of the samples collected in the plume at PANAMAX (Figure 4) or at depth at station 2 (Figure 7) with that of the TA standard, the characteristic reduction wave at -0.04 V is missing, indicating that TA is not present in significant concentrations in any of those samples. The $RSS^{2}_{-0.18\ V}$ signal detected at low pH is therefore due to other RSS compounds whose peak potential is the same as TA in acidic conditions. $RSS^{2}_{-0.18\ V}$ compounds (often referred to as TA-like compounds) have been observed in estuarine and river waters (Marie et al., 2017, 2015; Superville et al., 2013) and phytoplankton have also been shown to exude a RSS electrochemically similar to TA (Leal et al., 1999). However, TA is not known to be present in marine environments and is toxic to marine organisms with concentrations of 50 nM causing inhibition of growth in phytoplankton (Vasconcelos et al., 2002). In contrast to TA, GSH is thought to be common in marine waters (Dupont et al., 2006; Kading, 2013; Tang et al., 2000). The shape of the pseudopolarograms from PANAMAX (depth 181 m) and station 8 (surface at 25 m) were similar to that of GSH (Figures 4 and 6 respectively). While pseudopolarography cannot provide the exact identification of the RSS present, it can provide interesting details on the behaviour of various RSS that exist in the marine environment.

5 Conclusion

This study provides a quantitative and qualitative data set of species-specific RSS ($RSS^{2}_{-0.18\ V}$ and GSH-like compounds) in the WTSP Ocean. We find RSS are ubiquitous in the WTSP and concentrations are higher in the Melanesian waters and Lau basins than in the South Pacific Gyre, most likely because of sources linked to hydrothermal activity. Vertical profiles of $RSS^{2}_{-0.18\ V}$ and GSH-like compounds suggest a combination of distinct and common processes drive their biogeochemical cycling. $RSS^{2}_{-0.18\ V}$ compounds were detected in all sampled depths, while GSH-like compounds were confined to the upper 200 m, with both showing some evidence of photodegradation. Hydrothermal influence was particularly evident at the PANAMAX site, the only site where sulfide was detected (within a hydrothermal plume sample). Relatively high concentrations of $RSS^{2}_{-0.18\ V}$ and GSH-like compounds were also obtained in the hydrothermal plume, possibly due to a mixture of biotic and abiotic processes. Station 2 in the Melanesian Basin also saw elevated concentrations of $RSS^{2}_{-0.18\ V}$ compounds relative to other stations excluding the hydrothermal station, along the entire water column and at depth. The elevated concentrations suggest the production of these compounds, likely through unidentified local hydrothermal input, or possibly through *in-situ* production at this station.

Pseudopolarography of $RSS^{8.5}_{-0.52\ V}$ highlights the diversity of RSS compounds present in water. Most samples selected for pseudopolarography did not show a characteristic wave for TA suggesting that the $RSS^{2}_{-0.18\ V}$ signal detected in acidic conditions in these samples is not TA, while pseudopolarography supported the presence of GSH. Pseudopolarograms varied significantly between samples and highlighted the presence of various RSS substances, based on the variation and shape of the pseudopolarographic wave. While voltammetry is always prone to coalescence of peaks, pseudopolarography may be used as a tool to identify, and possibly quantify, some RSS species but this is a challenging task if many unknown RSS are present altogether. Studying the chemical stability of these RSS in relation to their reduction wave potential might provide further insights into their identity and biogeochemical cycling.

Data availability statement

The datasets presented in this study can be found in online repositories. The names of the repository/repositories and accession number(s) can be found below: http://www.obs-vlfr.fr/proof/php/TONGA/tonga.php#SA.

Author contributions

GP: Writing – original draft, Writing – review & editing, Investigation. HW: Supervision, Writing – review & editing. PS: Supervision, Writing – review & editing.

Funding

The author(s) declare financial support was received for the research, authorship, and/or publication of this article. The work presented in this publication was funded by the Natural Environment Research Council (NERC) EAO Doctoral Training Partnership (grant NE/L002469/1). This work contributes to the TONGA project (Shallow hydrothermal sources of trace elements: possible consequences on biological productivity and the biological carbon pump). The TONGA cruise (GEOTRACES GPpr14, November 2019, https://doi.org/10.17600/18000884) was funded by the TGIR Flotte Océanographique Française, the A-MIDeX foundation of Aix-Marseille University, the LEFE-CYBER and GMMC programs, and the ANR (grant TONGA ANR-18- CE01-0016). This work was partially supported by the "PHC Alliance" programme, funded by the UK Department for Business, Energy & Industrial Strategy (now DSIT), the French Ministry for Europe and Foreign Affairs, and the French Ministry of Higher Education, Research and Innovation. The International GEOTRACES

Programme is possible in part thanks to the support from the U.S. National Science Foundation (OCE-2140395) to the Scientific Committee on Oceanic Research (SCOR).

Acknowledgments

We warmly thank the scientific team, the captain, and the crew of the R/V L'Atalante for their cooperative efforts at sea throughout the TONGA cruise. We thank the members of the trace metal sample team, and V. Taillander for the CTD acquisition and data treatment. We also acknowledge S. Bonnet for her helpful input on the manuscript.

Conflict of interest

The authors declare that the research was conducted in the absence of any commercial or financial relationships that could be construed as a potential conflict of interest.

The reviewer RB declared a past co-authorship with the author HW to the handling editor.

Publisher's note

Supplementary material

The Supplementary Material for this article can be found online at: https://www.frontiersin.org/articles/10.3389/fmars.2024.1426906/full#supplementary-material

References

Ahner, B., Wei, L., Oleson, J., and Ogura, N. (2002). Glutathione and other low molecular weight thiols in marine phytoplankton under metal stress. *Mar. Ecol. Prog. Ser.* 232, 93–103. doi: 10.3354/meps232093

Al-Farawati, R., and van den Berg, C. M. G. (1997). The determination of sulfide in seawater by flow-analysis with voltammetric detection. *Mar. Chem.* 57, 277–286. doi: 10.1016/S0304-4203(97)00014-5

Al-Farawati, R., and van den Berg, C. M. G. (2001). Thiols in coastal waters of the western North Sea and English Channel. *Environ. Sci. Technol.* 35, 1902–1911. doi: 10.1021/es000073i

Aparicio-González, A., Duarte, C. M., and Tovar-Sánchez, A. (2012). Trace metals in deep ocean waters: A review. *J. Mar. Syst.* 100–101, 26–33. doi: 10.1016/j.jmarsys.2012.03.008

Apel, K., and Hirt, H. (2004). REACTIVE OXYGEN SPECIES: metabolism, oxidative stress, and signal transduction. *Annu. Rev. Plant Biol.* 55, 373–399. doi: 10.1146/annurev.arplant.55.031903.141701

Ardyna, M., Lacour, L., Sergi, S., d'Ovidio, F., Sallée, J.-B., Rembauville, M., et al. (2019). Hydrothermal vents trigger massive phytoplankton blooms in the Southern Ocean. *Nat. Commun.* 10, 2451. doi: 10.1038/s41467-019-09973-6

Aumond, V., Waeles, M., Salaün, P., Gibbon-Walsh, K., van den Berg, C. M. G., Sarradin, P.-M., et al. (2012). Sulfide determination in hydrothermal seawater samples using a vibrating gold micro-wire electrode in conjunction with stripping chronopotentiometry. *Anal. Chim. Acta* 753, 42–47. doi: 10.1016/j.aca.2012.09.044

Baba, S. P., and Bhatnagar, A. (2018). Role of thiols in oxidative stress. *Curr. Opin. Toxicol.* 7, 133–139. doi: 10.1016/j.cotox.2018.03.005

Baker, E. T., Massoth, G. J., and Feely, R. A. (1987). Cataclysmic hydrothermal venting on the Juan de Fuca Ridge. *Nature* 329, 149–151. doi: 10.1038/329149a0

Baker, E. T., Walker, S. L., Massoth, G. J., and Resing, J. A. (2019). The NE Lau Basin: Widespread and abundant hydrothermal venting in the back-arc region behind a superfast subduction zone. *Front. Mar. Sci.* 6. doi: 10.3389/fmars.2019.00382

Baumberger, T., Lilley, M. D., Lupton, J. E., Baker, E. T., Resing, J. A., Buck, N. J., et al. (2020). Dissolved gas and metal composition of hydrothermal plumes from a 2008 submarine eruption on the northeast lau spreading center. *Front. Mar. Sci.* 7. doi: 10.3389/fmars.2020.00171

Benavides, M., Bonnet, S., Le Moigne, F. A. C., Armin, G., Inomura, K., Hallstrøm, S., et al. (2022). Sinking Trichodesmium fixes nitrogen in the dark ocean. *ISME J.* 16, 2398–2405. doi: 10.1038/s41396-022-01289-6

Benavides, M., Conradt, L., Bonnet, S., Berman-Frank, I., Barrillon, S., Petrenko, A., et al. (2021). Fine-scale sampling unveils diazotroph patchiness in the South Pacific Ocean. *ISME Commun.* 1. doi: 10.1038/s43705-021-00006-2

Bendel, V., Fouquet, Y., Auzende, J.-M., Lagabrielle, Y., Grimaud, D., and Urabe, T. (1993). The White Lady hydrothermal field, North Fiji back-arc basin, Southwest Pacific. *Economic Geology* 88, 2237–2245. doi: 10.2113/gsecongeo.88.8.2237

Bi, Z., Salaün, P., and van den Berg, C. M. G. (2013). Determination of lead and cadmium in seawater using a vibrating silver amalgam microwire electrode. *Anal. Chim. Acta* 769, 56–64. doi: 10.1016/j.aca.2013.01.049

Bjørklund, G., Crisponi, G., Nurchi, V. M., Cappai, R., Djordjevic, A. B., and Aaseth, J. (2019). A review on coordination properties of thiol-containing chelating agents towards mercury, cadmium, and lead. *Molecules.* 24, 3247. doi: 10.3390/molecules24183247

Bluhm, K., Croot, P., Wuttig, K., and Lochte, K. (2010). Transformation of iodate to iodide in marine phytoplankton driven by cell senescence. *Aquat Biol.* 11, 1–15. doi: 10.3354/ab00284

Bocian-Ostrzycka, K. M., Grzeszczuk, M. J., Banaś, A. M., and Jagusztyn-Krynicka, E. K. (2017). Bacterial thiol oxidoreductases — from basic research to new antibacterial strategies. *Appl. Microbiol. Biotechnol.* 101, 3977–3989. doi: 10.1007/s00253-017-8291-8

Bonnet, S., Benavides, M., Le Moigne, F. A. C., Camps, M., Torremocha, A., Grosso, O., et al. (2023b). Diazotrophs are overlooked contributors to carbon and nitrogen export to the deep ocean. *ISME J.* 17, 47–58. doi: 10.1038/s41396-022-01319-3

Bonnet, S., Caffin, M., Berthelot, H., Grosso, O., Benavides, M., Helias-Nunige, S., et al. (2018). In-depth characterization of diazotroph activity across the western tropical South Pacific hotspot of N2 fixation (OUTPACE cruise). *Biogeosciences* 15, 4215–4232. doi: 10.5194/bg-15-4215-2018

Bonnet, S., Caffin, M., Berthelot, H., and Moutin, T. (2017). Hotspot of N2 fixation in the western tropical South Pacific pleads for a spatial decoupling between N2 fixation and denitrification. *PNAS* 114, E2800–E2801. doi: 10.17600/15000900

Bonnet, S., Guieu, C., Taillandier, V., Boulart, C., Bouruet-Aubertot, P., Gazeau, F., et al. (2023a). Natural iron fertilization by shallow hydrothermal sources fuels diazotroph blooms in the ocean. *Science 1979* 380, 812–817. doi: 10.1126/science.abq4654

Brand, L. E., Sunda, W. G., and Guillard, R. R. L. (1986). Reduction of marine phytoplankton reproduction rates by copper and cadmium. *J. Exp. Mar. Biol. Ecol.* 96, 225–250. doi: 10.1016/0022-0981(86)90205-4

Butler, E. A., Peters, D. G., and Swift, E. H. (1958). Hydrolysis reactions of thioacetamide in aqueous solutions. *Anal. Chem.* 30, 1379–1383. doi: 10.1021/ac60140a027

Caffin, M., Moutin, T., Ann Foster, R., Bouruet-Aubertot, P., Michelangelo Doglioli, A., Berthelot, H., et al. (2018). N2 fixation as a dominant new N source in the western tropical South Pacific Ocean (OUTPACE cruise). *Biogeosciences* 15, 2565–2585. doi: 10.5194/bg-15-2565-2018

Cameron, J. C., and Pakrasi, H. B. (2011). Glutathione facilitates antibiotic resistance and photosystem I stability during exposure to gentamicin in cyanobacteria. *Appl. Environ. Microbiol.* 77, 3547–3550. doi: 10.1128/AEM.02542-10

Carfagna, S., Bottone, C., Cataletto, P. R., Petriccione, M., Pinto, G., Salbitani, G., et al. (2016). Impact of sulfur starvation in autotrophic and heterotrophic cultures of the extremophilic microalga galdieria phlegrea (Cyanidiophyceae). *Plant Cell Physiol.* 57, 1890–1898. doi: 10.1093/pcp/pcw112

Carrillo, A., Mota, M. L., Carrasco, L. A., Cruz, E. C., Luque, P. A., Mireles, M. C., et al. (2018). Low-Temperature synthesis of CdS and ZnS nanoparticles by solution method using an anionic surfactant. *Chalcogenide Lett.* 15, 565–571.

Chapman, C. S., Capodaglio, G., Turetta, C., and van den Berg, C. M. G. (2009). Benthic fluxes of copper, complexing ligands and thiol compounds in shallow lagoon waters. *Mar. Environ. Res.* 67, 17–24. doi: 10.1016/j.marenvres.2008.07.010

Chu, C., Stamatelatos, D., and McNeill, K. (2017). Aquatic indirect photochemical transformations of natural peptidic thiols: impact of thiol properties, solution pH, solution salinity and metal ions. *Environ. Sci. Process Impacts* 19, 1518–1527. doi: 10.1039/C7EM00324B

Ciglenečki, I., and Ćosović, B. (1996). Electrochemical study of sulfur species in seawater and marine phytoplankton cultures. *Mar. Chem* 52, 87–97. doi: 10.1016/0304-4203(95)00080-1

Cotte, L., Omanović, D., Waeles, M., Laës, A., Cathalot, C., Sarradin, P. M., et al. (2018). On the nature of dissolved copper ligands in the early buoyant plume of hydrothermal vents. *Environ. Chem.* 15, 58–73. doi: 10.1071/EN17150

Courbot, M., Diez, L., Ruotolo, R., Chalot, M., and Leroy, P. (2004). Cadmium-responsive thiols in the ectomycorrhizal fungus Paxillus involutus. *Appl. Environ. Microbiol.* 70, 7413–7417. doi: 10.1128/AEM.70.12.7413-7417.2004

Cutter, G., Casciotti, K., Croot, P., Geibert, W., Geochemistry, M., Heimbürger, L.-E., et al. (2017). *Sampling and sample-handling protocols for GEOTRACES cruises*.

Damm, K. L., Oosting, S. E., Kozlowski, R., Buttermore, L. G., Colodner, D. C., Edmonds, H. N., et al. (1995). Evolution of East Pacific Rise hydrothermal vent fluids following a volcanic eruption. *Nature* 375, 47–50. doi: 10.1038/375047a0

Dias, D., do Nascimento, P. C., Jost, C. L., Bohrer, D., de Carvalho, L. M., and Koschinsky, A. (2010). Voltammetric determination of low-molecular-weight sulfur compounds in hydrothermal vent fluids – studies with hydrogen sulfide, methanethiol, ethanethiol and propanethiol. *Electroanalysis* 22, 1066–1071. doi: 10.1002/elan.200900472

Dulaquais, G., Fourrier, P., Guieu, C., Mahieu, L., Riso, R., Salaun, P., et al. (2023). The role of humic-type ligands in the bioavailability and stabilization of dissolved iron in the Western Tropical South Pacific Ocean. *Front. Mar. Sci.* 10. doi: 10.3389/fmars.2023.1219594

Dupont, C. L., and Ahner, B. A. (2005). Effects of copper, cadmium, and zinc on the production and exudation of thiols by Emiliania huxleyi. *Limnol. Oceanogr.* 50, 508–515. doi: 10.4319/lo.2005.50.2.0508

Dupont, C. L., Moffett, J. W., Bidigare, R. R., and Ahner, B. A. (2006). Distributions of dissolved and particulate biogenic thiols in the subartic Pacific Ocean. *Deep Sea Res. 1 Oceanogr. Res. Pap.* 53, 1961–1974. doi: 10.1016/j.dsr.2006.09.003

Dupont, C. L., Nelson, R. K., Bashir, S., Moffett, J. W., and Ahner, B. A. (2004). Novel copper-binding and nitrogen-rich thiols produced and exuded by Emiliania huxleyi. *Limnol. Oceanogr.* 49, 1754–1762. doi: 10.4319/lo.2004.49.5.1754

Farr, J. P. G., and Laditan, G. O. A. (1974a). The polarography of molybdate in the presence of organic sulphur and nitrogen compounds part II. The polarographic estimation of molybdenum (VI) with thioacetamide. . *J. Less Common Metals* 36, 161–168. doi: 10.1016/0022-5088(74)90095-2

Farr, J. P. G., and Laditan, G. O. A. (1974b). The polarography of molybdate in the presence of organic sulphur and nitrogen compounds part I. The electrochemical behaviour of aqueous acidified solutions of ammonium molybdate with thioacetamide. *J. Less Common Metals* 36, 151–160. doi: 10.1016/0022-5088(74)90094-0

Feely, R. A., Baker, E. T., Marumo, I. K., Urabe, T., ISHIBASHI, J., Gendron, J., et al. (1996). Hydrothermal plume particles and dissolved phosphate over the superfast-spreading southern East Pacific Rise. *Geochim. Cosmochim. Acta* 60, 2297–2323. doi: 10.1016/0016-7037(96)00099-3

Findlay, A. J., Estes, E. R., Gartman, A., Yücel, M., Kamyshny, A., and Luther, G. W. (2019). Iron and sulfide nanoparticle formation and transport in nascent hydrothermal vent plumes. *Nat. Commun.* 10, 1597. doi: 10.1038/s41467-019-09580-5

Fourrier, P., and Dulaquais, G. (2024). Low-molecular-weight reduced sulfur substances: A major component of nonvolatile dissolved organic sulfur in the Pacific Ocean. *Limnol Oceanogr Lett*. doi: 10.1002/lol2.10417

Foustoukos, D. I., Allen, D. E., Fu, Q., and Seyfried, W. E. (2001). "Experimental study of CO2(aq)/CO(aq) redox equilibria at elevated temperatures and pressures: The effect of pH on reaction relations," in *Goldschmidt Conference*.

Gao, Z., and Guéguen, C. (2018). Distribution of thiol, humic substances and colored dissolved organic matter during the 2015 Canadian Arctic GEOTRACES cruises. *Mar. Chem.* 203, 1–9. doi: 10.1016/j.marchem.2018.04.001

German, C. R., Baker, E. T., Connelly, D. P., Lupton, J. E., Resing, J., Prien, R. D., et al. (2006). Hydrothermal exploration of the fonualei rift and spreading center and the northeast lau spreading center. *Geochemistry Geophysics Geosystems* 7, 1-15. doi: 10.1029/2006GC001324

Giovanelli, J. (1987). Sulfur amino acids of plants: an overview. *Methods Enzymol.* 143, 419–426. doi: 10.1016/0076-6879(87)43073-5

Gomez-Saez, G. V., Dittmar, T., Holtappels, M., Pohlabeln, A. M., Lichtschlag, A., Schnetger, B., et al. (2021). Sulfurization of dissolved organic matter in the anoxic water column of the Black Sea. *Sci. Adv.* 7. doi: 10.1126/sciadv.abf6199

Gomez-Saez, G. V., Pohlabeln, A. M., Stubbins, A., Marsay, C. M., and Dittmar, T. (2017). Photochemical alteration of dissolved organic sulfur from sulfidic porewater. *Environ. Sci. Technol.* 51, 14144–14154. doi: 10.1021/acs.est.7b03713

Guieu, C., and Bonnet, S. (2019). *TONGA 2019 cruise, R/V L'Atalante [WWW document]*. doi: 10.17600/18000884

Guieu, C., Bonnet, S., Petrenko, A., Menkes, C., Chavagnac, V., Desboeufs, K., et al. (2018). Iron from a submarine source impacts the productive layer of the Western Tropical South Pacific (WTSP). *Sci. Rep.* 8, 1-9. doi: 10.1038/s41598-018-27407-z

Hannington, M. D., De Ronde, C. E. J., and Petersen, S. (2005). "Sea-floor tectonics and submarine hydrothermal systems," in *Economic geology 100th anniversary*, 111–141. doi: 10.5382/av100.06

Harris, D. C. (2010). *Quantitative chemical analysis. 8th edition* (New York: W.H. Freeman and Company), 108.

Heinen, W., and Lauwers, A. M. (1996). Organic sulfur compounds resulting from the interaction of iron sulfide, hydrogen sulfide and carbon dioxide in an anaerobic aqueous environment. *Origins Life Evol. Biospheres* 26, 131–150. doi: 10.1007/BF01809852

Hodgkinson, M. R. S., Webber, A. P., Roberts, S., Mills, R. A., Connelly, D. P., and Murton, B. J. (2015). Talc-dominated seafloor deposits reveal a new class of hydrothermal system. *Nat. Commun.* 6, 10150. doi: 10.1038/ncomms10150

Howard, P. H., Boethling, R. S., Jarvis, W. F., Meylan, W. M., and Michalenko, E. M. (2017). *Handbook of environmental degradation rates* (CRC Press). doi: 10.1201/9780203719329

Hsu-Kim, H., Mullaugh, K. M., Tsang, J. J., Yucel, M., and Luther, G. W. (2008). Formation of Zn- and Fe-sulfides near hydrothermal vents at the Eastern Lau Spreading Center: Implications for sulfide bioavailability to chemoautotrophs. *Geochem. Trans.* 9, 1-14. doi: 10.1186/1467-4866-9-6

Hu, H., Mylon, S. E., and Benoit, G. (2006). Distribution of the thiols glutathione and 3-mercaptopropionic acid in Connecticut lakes. *Limnol. Oceanogr.* 51, 2763–2774. doi: 10.4319/lo.2006.51.6.2763

Huang, X. G., Li, S., Liu, F. J., and Lan, W. R. (2018). Regulated effects of Prorocentrum donghaiense Lu exudate on nickel bioavailability when cultured with different nitrogen sources. *Chemosphere* 197, 57–64. doi: 10.1016/j.chemosphere.2018.01.014

Jeng, H.-M., Tsai, C.-Z., and Chang, T.-Y. (1990). Voltammetric study of copper(I) thioacetamide complexes. *Fresenius J. Anal. Chem.* 338, 902–904. doi: 10.1007/BF00322029

Kading, T. (2013). Distribution of thiols in the northwest Atlantic Ocean (Thesis). Massachusetts: Massachusetts Institute of Technology and Woods Hole Oceanographic Institution. doi: 10.1575/1912/5711

Kalloniati, C., Krompas, P., Karalias, G., Udvardi, M. K., Rennenberg, H., Herschbach, C., et al. (2015). Nitrogen-fixing nodules are an important source of reduced sulfur, which triggers global changes in sulfur metabolism in lotus japonicus. *Plant Cell* 27, 2384–2400. doi: 10.1105/tpc.15.00108

Kawakami, S., Gledhill, M., and Achterberg, E. (2006). Determination of phytochelatins and glutathione in phytoplankton from natural waters using HPLC with fluorescence detection. *TrAC Trends Analytical Chem.* 25, 133–142. doi: 10.1016/j.trac.2005.06.005

Kiene, R. P. (1991). Evidence for the biological turnover of thiols in anoxic marine sediments. *Biogeochemistry* 13, 117–135. doi: 10.1007/BF00002773

Kiene, R. P., Malloy, K. D., and Taylor, B. F. (1990). Sulfur-containing amino acids as precursors of thiols in anoxic coastal sediments. *Appl. Environ. Microbiol.* 56, 156–161. doi: 10.1128/aem.56.1.156-161.1990

Kleint, C., Kuzmanovski, S., Powell, Z., Bühring, S. I., Sander, S. G., and Koschinsky, A. (2015). Organic Cu-complexation at the shallow marine hydrothermal vent fields off the coast of Milos (Greece), Dominica (Lesser Antilles) and the Bay of Plenty (New Zealand). *Mar. Chem.* 173, 244–252. doi: 10.1038/269319a0

Klinhammer, G., Bender, M., and Weiss, R. F. (1977). Hydrothermal manganese in the Galapagos Rift. *Nature* 269, 319–320. doi: 10.1038/269319a0

Klinkhammer, G., Elderfield, H., and Hudsont, A. (1983). Rare earth elements in seawater near hydrothermal vents. *Nature* 305, 185–188. doi: 10.1038/305185a0

Konn, C., Charlou, J. L., Donval, J. P., Holm, N. G., Dehairs, F., and Bouillon, S. (2009). Hydrocarbons and oxidized organic compounds in hydrothermal fluids from Rainbow and Lost City ultramafic-hosted vents. *Chem. Geol.* 258, 299–314. doi: 10.1016/j.chemgeo.2008.10.034

Kumar, V., Pandita, S., Singh Sidhu, G. P., Sharma, A., Khanna, K., Kaur, P., et al. (2021). Copper bioavailability, uptake, toxicity and tolerance in plants: A comprehensive review. *Chemosphere* 262, 127810. doi: 10.1016/j.chemosphere.2020.127810

Laglera, L. M., Downes, J., Tovar-Sánchez, A., and Monticelli, D. (2014). Cathodic pseudopolarography: A new tool for the identification and quantification of cysteine, cystine and other low molecular weight thiols in seawater. *Anal. Chim. Acta* 836, 24–33. doi: 10.1016/j.aca.2014.05.026

Laglera, L. M., and Tovar-Sánchez, A. (2012). Direct recognition and quantification by voltammetry of thiol/thioamide mixes in seawater. *Talanta* 89, 496–504. doi: 10.1016/j.talanta.2011.12.075

Laglera, L. M., and van den Berg, C. M. G. (2006). Photochemical oxidation of thiols and copper complexing ligands in estuarine waters. *Mar. Chem.* 101, 130–140. doi: 10.1016/j.marchem.2006.01.006

Lang, S. Q., Butterfield, D. A., Schulte, M., Kelley, D. S., and Lilley, M. D. (2010). Elevated concentrations of formate, acetate and dissolved organic carbon found at the Lost City hydrothermal field. *Geochim. Cosmochim. Acta* 74, 941–952. doi: 10.1016/j.gca.2009.10.045

Leal, M. F. C., and van den Berg, C. M. G. (1998). Evidence for strong copper(I) complexation by organic ligands in seawater. *Aquat. Geochemistry* 4, 49–75. doi: 10.1023/A:1009653002399

Leal, M. F. C., Vasconcelos, M. T. S. D., and van den Berg, C. M. G. (1999). Copper-induced release of complexing ligands similar to thiols by Emiliania huxleyi inseawater cultures. *Limnol. Oceanogr.* 44, 1750–1762. doi: 10.4319/lo.1999.44.7.1750

Le Gall, A. C., and van den Berg, C. M. G. (1998). Folic acid and glutathione in the water column of the North East Atlantic. *Deep Sea Res. Part I: Oceanographic Res. Papers* 45, 1903–1918. doi: 10.1016/S0967-0637(98)00042-9

Lohan, M. C., and Tagliabue, A. (2018). Oceanic micronutrients: Trace metals that are essential for marine life. *Elements* 14, 385-390. doi: 10.2138/gselements.14.6.385

Madkour, L. H. (2020a). Oxidative stress and oxidative damage-induced cell death, in: Reactive Oxygen Species (ROS), Nanoparticles, and Endoplasmic Reticulum (ER) Stress-Induced Cell Death Mechanisms. *Elsevier* pp, 175–197. doi: 10.1016/b978-0-12-822481-6.00008-6

Madkour, L. H. (2020b). "Biological mechanisms of reactive oxygen species (ROS)," in *Reactive oxygen species (ROS), nanoparticles, and endoplasmic reticulum (ER) stress-induced cell death mechanisms* (Elsevier), 19–35. doi: 10.1016/b978-0-12-822481-6.00002-5

Mahieu, L., Whitby, H., Dulaquais, G., Tilliette, C., Guigue, C., Lefevre, D., et al. (2024). Iron-binding by dissolved organic matter in the Western Tropical South Pacific Ocean (GEOTRACES TONGA cruise GPpr14). *Front. Mar. Sci.* 11. doi: 10.1021/ba-1968-0073.ch017

Mallory, E. C. (1968). A thioacetamide-precipitation procedure for determining trace elements in water, in: trace inorganics in water. *Adv. Chem.* 17, 281–295. doi: 10.1021/ba-1968-0073.ch017

Mangal, V., Phung, T., and Guéguen, C. (2020). An estimation of sulfur concentrations released by three algae (Chlorella vulgaris, Chlamydomonas reinhardtii, Scenedesmus obliquus) in response to variable growth photoperiods. *Environ. Sci. pollut. Res.* 27, 12491–12498. doi: 10.1007/s11356-020-07812-6

Marie, L., Pernet-Coudrier, B., Waeles, M., Gabon, M., and Riso, R. (2015). Dynamics and sources of reduced sulfur, humic substances and dissolved organic carbon in a temperate river system affected by agricultural practices. *Sci. Total Environ.* 537, 23–32. doi: 10.1016/j.scitotenv.2015.07.089

Marie, L., Pernet-Coudrier, B., Waeles, M., and Riso, R. (2017). Seasonal variation and mixing behaviour of glutathione, thioacetamide and fulvic acids in a temperate macrotidal estuary (Aulne, NW France). *Estuar. Coast. Shelf Sci.* 184, 177–190. doi: 10.1016/j.ecss.2016.11.018

McCollom, T. M., and Seewald, J. S. (2007). Abiotic synthesis of organic compounds in deep-sea hydrothermal environments. *Chem. Rev.* 107, 382–401. doi: 10.1021/cr0503660

McLeay, Y., Stannard, S., Houltham, S., and Starck, C. (2017). Dietary thiols in exercise: Oxidative stress defence, exercise performance, and adaptation. *J. Int. Soc Sports Nutr.* 14, 1-8. doi: 10.1186/s12970-017-0168-9

Mironov, I. V., and Tsvelodub, L. D. (1996). Complexation of copper(I) by thiourea in acidic aqueous solution. *J. Solution Chem.* 25, 315–325. doi: 10.1007/BF00972529

Moingt, M., Bressac, M., Bélanger, D., and Amyot, M. (2010). Role of ultra-violet radiation, mercury and copper on the stability of dissolved glutathione in natural and artificial freshwater and saltwater. *Chemosphere* 80, 1314–1320. doi: 10.1016/j.chemosphere.2010.06.041

Moore, J. K., Doney, S. C., Glover, D. M., and Fung, I. Y. (2001). Iron cycling and nutrient-limitation patterns in surface waters of the World Ocean. *Deep Sea Res. Part II: Topical Stud. Oceanography* 49, 463–507. doi: 10.1016/S0967-0645(01)00109-6

Moore, C. M., Mills, M. M., Arrigo, K. R., Berman-Frank, I., Bopp, L., Boyd, P. W., et al. (2013). Processes and patterns of oceanic nutrient limitation. *Nat. Geosci.* 6, 701–710. doi: 10.1038/ngeo1765

Mopper, K., and Kieber, D. J. (1991). Distribution and biological turnover of dissolved organic compounds in the water column of the Black Sea. *Deep Sea Res. Part A. Oceanographic Res. Papers* 38, S1021–S1047. doi: 10.1016/S0198-0149(10)80022-6

Moran, M. A., and Durham, B. P. (2019). Sulfur metabolites in the pelagic ocean. *Nat. Rev. Microbiol.* 17, 665–678. doi: 10.1038/s41579-019-0250-1

Morel, F. M. M., and Price, N. M. (2003). The biogeochemical cycles of trace metals in the oceans. *Science* 300, 944–947. doi: 10.1126/science.1083545

Morelli, E., and Scarano, G. (2004). Copper-induced changes of non-protein thiols and antioxidant enzymes in the marine microalga Phaeodactylum tricornutum. *Plant Sci.* 167, 289–296. doi: 10.1016/j.plantsci.2004.04.001

Morris, J. J., Rose, A. L., and Lu, Z. (2022). Reactive oxygen species in the world ocean and their impacts on 980 marine ecosystems. *Redox Biol.* 52, 102285. doi: 10.1016/j.redox.2022.102285

Navarrete, A., González, A., Gómez, M., Contreras, R. A., Díaz, P., Lobos, G., et al. (2019). Copper excess detoxification is mediated by a coordinated and complementary induction of glutathione, phytochelatins and metallothioneins in the green seaweed Ulva compressa. *Plant Physiol. Biochem.* 135, 423–431. doi: 10.1016/j.plaphy.2018.11.019

Nojiri, Y., Ishibashi, J., Kawai, T., Otsuki, A., and Sakai, H. (1989). Hydrothermal plumes along the North Fiji Basin spreading axis. *Nature* 342, 667–670. doi: 10.1038/342667a0

Omanovic, D., and Branica, M. (1998). Automation of voltammetric measurements by polarographic analyser PAR 384B*. *Croatica Chemica Acta* 71, 421–433.

Pál, M., Janda, T., and Szalai, G. (2018). Interactions between plant hormones and thiol-related heavy metal chelators. *Plant Growth. Regul.* 85, 17–185. doi: 10.1007/s10725-018-0391-7

Pernet-Coudrier, B., Waeles, M., Filella, M., Quentel, F., and Riso, R. D. (2013). Simple and simultaneous determination of glutathione, thioacetamide and refractory organic matter in natural waters by DP-CSV. *Sci. Total Environ.* 463–464, 997–1005. doi: 10.1016/j.scitotenv.2013.06.053

Peters, C., Strauss, H., Haase, K., Bach, W., de Ronde, C. E. J., Kleint, C., et al. (2021). SO2 disproportionation impacting hydrothermal sulfur cycling: Insights from multiple sulfur isotopes for hydrothermal fluids from the Tonga-Kermadec intraoceanic arc and the NE Lau Basin. *Chem. Geol* 586, 120586. doi: 10.1016/j.chemgeo.2021.120586

Petzold, H., and Sadler, P. J. (2008). Oxidation induced by the antioxidant glutathione (GSH). *Chem. Comm.* 37, 4413–4415. doi: 10.1039/b805358h

Portlock, G., Fourrier, P., Riso, R., Omanovic, D., Dulaquais, G., Whitby, H., et al. Humic substances in the oligotrophic western tropical South Pacific: an intercomparison of electrochemical techniques.

Radford-Knoery, J., Charlou, J.-L., Donval, J.-P., Aballéa, M., Fouquet, Y., and Ondréas, H. (1998). Distribution of dissolved sulfide, methane, and manganese near the seafloor at the Lucky Strike (37°17′N) and Menez Gwen (37°50′N) hydrothermal vent sites on the mid-Atlantic Ridge. *Deep Sea Res. Part I: Oceanographic Res. Papers* 45, 367–386. doi: 10.1016/S0967-0637(97)00082-4

Rea, P. A., Vatamaniuk, O. K., and Rigden, D. J. (2004). Weeds, worms, and more. Papain's long-lost cousin, phytochelatin synthase. *Plant Physiol.* 136, 2463–2474. doi: 10.1104/pp.104.048579

Reeves, E. P., McDermott, J. M., and Seewald, J. S. (2014). The origin of methanethiol in midocean ridge hydrothermal fluids. *Proc. Natl. Acad. Sci. U.S.A.* 111, 5474–5479. doi: 10.1073/pnas.1400643111

Resing, J. A., Sedwick, P. N., German, C. R., Jenkins, W. J., Moffett, J. W., Sohst, B. M., et al. (2015). Basin-scale transport of hydrothermal dissolved metals across the South Pacific Ocean. *Nature* 523, 200–203. doi: 10.1038/nature14577

Rijstenbil, J. W. (2002). Assessment of oxidative stress in the planktonic diatom Thalassiosira pseudonana in response to UVA and UVB radiation. *J. Plankton. Res.* 24, 1277–1288. doi: 10.1093/plankt/24.12.1277

Rosenthal, D., and Taylor, T. I. (1957). A study of the mechanism and kinetics of the thioacetamide hydrolysis reaction 1. *J. Am. Chem. Soc.* 79, 2684–2690. doi: 10.1021/ja01568a007

Sander, S. G., and Koschinsky, A. (2011). Metal flux from hydrothermal vents increased by organic complexation. *Nat. Geosci.* 4, 145–150. doi: 10.1038/ngeo1088

Schäfer, H., and Eyice, Ö. (2019). "Microbial cycling of methanethiol," in *Methylotrophs and methylotroph communities* (Caister Academic Press). doi: 10.21775/9781912530045.09

Schieber, M., and Chandel, N. S. (2014). ROS function in redox signaling and oxidative stress. *Curr. Biol.* 24, R453–R462. doi: 10.1016/j.cub.2014.03.034

Schine, C. M. S., Alderkamp, A.-C., van Dijken, G., Gerringa, L. J. A., Sergi, S., Laan, P., et al. (2021). Massive Southern Ocean phytoplankton bloom fed by iron of possible hydrothermal origin. *Nat. Commun.* 12, 1211. doi: 10.1038/s41467-021-21339-5

Schlitzer, R. (2021). *Ocean data view*. [Software].

Schmidt, A., Erdle, I., and Köst, H.-P. (1982). Changes of C-Phycocyanin in Synechococcus 6301 in Relation to Growth on various Sulfur Compounds Materials and Methods. *Zeitschrift für Naturforschung C* 37, 870–876. doi: 10.1515/znc-1982-1004

Schulte, M. D., and Rogers, K. L. (2004). Thiols in hydrothermal solution: Standard partial molal properties and their role in the organic geochemistry of hydrothermal environments. *Geochim. Cosmochim. Acta* 68, 1087–1097. doi: 10.1016/j.gca.2003.06.001

Semeniuk, D. M., Bundy, R. M., Payne, C. D., Barbeau, K. A., and Maldonado, M. T. (2015). Acquisition of organically complexed copper by marine phytoplankton and bacteria in the northeast subarctic Pacific Ocean. *Mar. Chem.* 173, 222–233. doi: 10.1016/j.marchem.2015.01.005

Seyfried, W. E., Pester, N. J., Tutolo, B. M., and Ding, K. (2015). The Lost City hydrothermal system: Constraints imposed by vent fluid chemistry and reaction path models on subseafloor heat and mass transfer processes. *Geochim. Cosmochim. Acta* 163, 59–79. doi: 10.1016/j.gca.2015.04.040

Shao, Z., Xu, Y., Wang, H., Luo, W., Wang, L., Huang, Y., et al. (2023). Global oceanic diazotroph database version 2 and elevated estimate of global oceanic N2 fixation. *Earth Syst. Sci. Data* 15, 3673–3709. doi: 10.5194/essd-15-3673-2023

Steffens, J. C. (1990). The heavy metal-binding peptides of plants. *Annu. Rev. Plant Physiol. Plant Mol. Biol.* 41, 553–575. doi: 10.1146/annurev.pp.41.060190.003005

Stoffers, P., Worthington, T. J., Schwarz-Schampera, U., Hannington, M. D., Massoth, G. J., Hekinian, R., et al. (2006). Submarine volcanoes and high-temperature hydrothermal venting on the Tonga arc, southwest Pacific. *Geology* 34, 453–456. doi: 10.1130/G22227.1

Sunda, W., Kieber, D. J., Kiene, R. P., and Huntsman, S. (2002). An antioxidant function for DMSP and DMS in marine algae. *Nature* 418, 317–320. doi: 10.1038/nature00851

Superville, P. J., Pižeta, I., Omanović, D., and Billon, G. (2013). Identification and on-line monitoring of reduced sulphur species (RSS) by voltammetry in oxic waters. *Talanta* 112, 55–62. doi: 10.1016/j.talanta.2013.03.045

Swarr, G. J., Kading, T., Lamborg, C. H., Hammerschmidt, C. R., and Bowman, K. L. (2016). Dissolved low-molecular weight thiol concentrations from the U.S. GEOTRACES North Atlantic Ocean zonal transect. *Deep Sea Res. Part I: Oceanographic Res. Papers* 116, 77–87. doi: 10.1016/j.dsr.2016.06.003

Tang, D., Hung, C., Warnken, K. W., and Santschi, P. H. (2000). The distribution of biogenic thiols in surface waters of Galveston Bay. *Limnol. Oceanogr.* 45, 1289–1297. doi: 10.4319/lo.2000.45.6.1289

Tararin, L. A., Chubarov, K. M., and Filosofova, T. M. (2003). *Chemical composition of rock and minerals from the ophiolite complex in the Hunter Fracture Zone [WWW Document]* (PANGAEA).

Tilliette, C., Gazeau, F., Portlock, G., Benavides, M., Bonnet, S., Guigue, C., et al. (2023). Influence of shallow hydrothermal fluid release on the functioning of phytoplankton communities. *Front. Mar. Sci.* 10. doi: 10.3389/fmars.2023.1082077

Tilliette, C., Taillandier, V., Bouruet-Aubertot, P., Grima, N., Maes, C., Montanes, M., et al. (2022). Dissolved iron patterns impacted by shallow hydrothermal sources along a transect through the Tonga-kermadec arc. *Global Biogeochem Cycles* 36, 1-27. doi: 10.1029/2022GB007363

Treude, T., Smith, C. R., Wenzhöfer, F., Carney, E., Bernardino, A. F., Hannides, A. K., et al. (2009). Biogeochemistry of a deep-sea whale fall: Sulfate reduction, sulfide efflux and methanogenesis. *Mar. Ecol. Prog. Ser.* 382, 1–21. doi: 10.3354/meps07972

Ulrich, K., and Jakob, U. (2019). The role of thiols in antioxidant systems. *Free Radic. Biol. Med.* 140, 14–27. doi: 10.1016/j.freeradbiomed.2019.05.035

Umiker, K. J., Morra, M. J., and Francis Cheng, I. (2002). Aqueous sulfur species determination using differential pulse polarography. *Microchemical J.* 73, 287–297. doi: 10.1016/S0026-265X(02)00097-8

van den Berg, C. M. G. (1982). Determination of copper complexation with natural organic ligands in seawater by equilibration with MnO2 II. Experimental Procedures and Application to Surface Seawater. *Mar. Chem.* 11, 323–342. doi: 10.1016/0304-4203(82)90029-9

van den Berg, C. M. G., Household, B. C., and Riley, J. P. (1988). Determination of cystine and cysteine in seawater using cathodic stripping voltammetry in the presence of Cu(II). *J. Electroanal. Chem. Interfacial Electrochem.* 239, 137–148. doi: 10.1016/0022-0728(88)80275-4

Vasconcelos, M. T. S. D., and Leal, M. F. C. (2001). Adsorption and uptake of Cu by Emiliania huxleyi in natural seawater. *Environ. Sci. Technol.* 35, 508–515. doi: 10.1021/es000954p

Vasconcelos, M. T. S. D., Leal, M. F. C., and van den Berg, C. M. G. (2002). Influence of the nature of the exudates released by different marine algae on the growth, trace metal uptake and exudation of Emiliania huxleyi in natural seawater. *Mar. Chem.* 77, 187–210. doi: 10.1016/S0304-4203(01)00087-1

Walsh, E. A., Smith, D. C., Sogin, M. L., and D'Hondt, S. (2015). Bacterial and archaeal biogeography of the deep chlorophyll maximum in the South Pacific Gyre. *Aquat. Microb. Ecol.* 75, 1–13. doi: 10.3354/ame01746

Wang, H., Wang, W., Liu, M., Zhou, H., Ellwood, M. J., Butterfield, D. A., et al. (2022). Iron ligands and isotopes in hydrothermal plumes over backarc volcanoes in the Northeast Lau Basin, Southwest Pacific Ocean. *Geochim. Cosmochim. Acta* 336, 341–352. doi: 10.1016/j.gca.2022.09.026

Whitby, H., Posacka, A. M., Maldonado, M. T., and van den Berg, C. M. G. (2018). Copper-binding ligands in the NE pacific. *Mar. Chem.* 204, 36–48. doi: 10.1016/j.marchem.2018.05.008

Yeo, I. A., McIntosh, I. M., Bryan, S. E., Tani, K., Dunbabin, M., Metz, D., et al. (2022). The 2019–2020 volcanic eruption of Late'iki (Metis Shoal), Tonga. *Sci. Rep.* 12, 7468. doi: 10.1038/s41598-022-11133-8

Yücel, M., Gartman, A., Chan, C. S., and Luther, G. W. (2011). Hydrothermal vents as a kinetically stable source of iron-sulphide-bearing nanoparticles to the ocean. *Nat. Geosci.* 4, 367–371. doi: 10.1038/ngeo1148

Zhang, Z., Fan, W., Bao, W., Chen, C. T. A., Liu, S., and Cai, Y. (2020). Recent developments of exploration and detection of shallow-water hydrothermal systems. *Sustainability* 12, 1–17. doi: 10.3390/su12219109